

## Chapter 6 Building Response

In this chapter we will explore the nature of deformations and forces in buildings during earthquake shaking. Of course, buildings are complex connections of columns, beams, and walls, the study of which deserves an entire course in structural engineering. However, for our purposes, it is instructive to investigate the nature of forces and deformations that would occur in a solid body whose properties are similar to the average properties of a building. We begin with a simple description of different types of buildings and their characteristics. In general we will characterize buildings with the following parameters (refer to Figure 6.1).

- Density is important because it is used to calculate inertial momentum. The density of buildings ranges about  $100 \text{ kg/m}^3$  (tall flexible frame buildings) to  $200 \text{ kg/m}^3$  (stiff heavy shear wall buildings). Earthquake loads in buildings generally increase with the density of the building.
- Yield strength is maximum horizontal load that can be applied to a building. It is expressed in units of acceleration if the yield force is normalized by the weight of the building. While increasing yield strength is generally desirable, it usually comes with the penalty of increasing stiffness.
- Stiffness is the horizontal force distributed throughout a building divided by resulting lateral shear strain in the building (usually called drift). Maximum stresses in a building generally increases with stiffness, so making a building stiff can lead to high stresses. While low stiffness has advantages, decreasing stiffness usually comes with the penalties of increasing shear strains and decreasing yield strength.
- Ductility refers to the ratio of the horizontal shear strain at which a building collapses divided by the strain at which a building begins to strain inelastically. Increasing ductility is always desirable, but it usually comes with the penalty of increasing cost.

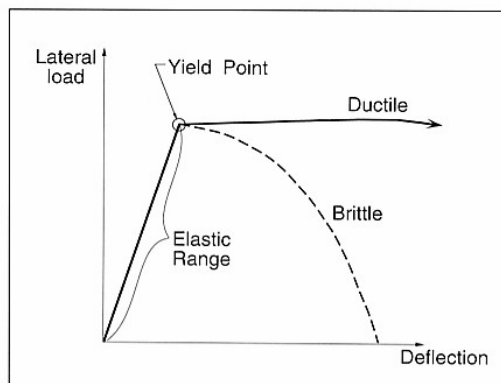


Figure 6.1 Idealized building response.

The following examples give some idea of different classes of buildings.

### **Concrete Shear-Wall Buildings**

This is a common class of buildings that generally have at least some walls that consist of continuous slabs of concrete. These concrete walls are very resistant to in plane shearing forces. Perpendicular shear walls are generally connected with each other through 1) the strong floor slabs, and 2) sometimes they are connected at corners of rooms. When a building consists of a rectangular concrete box with interior columns supporting the floor slab, then this is generally referred to box/shear-wall construction. This type of construction is very common at Caltech. It has the advantage of very high yield strength. Furthermore, if the walls are properly reinforced, the ductility is also high. This type of construction has the disadvantage that it tends to lead to very stiff buildings. As we see later in the chapter, this can lead to high stresses in a building. It also has the disadvantage that the architecture of the building is fixed. That is walls cannot be reconfigured once the building is constructed. Furthermore, because of their stiffness, it is impractical to build shear wall buildings taller than about 10 stories that also adequately resist earthquake loading.

Figure 6.2 shows two versions of the Olive View Hospital in the San Fernando Valley. The first version was a nonductile-concrete frame building that was completed just prior to its collapse in the 1971 San Fernando earthquake. The hospital was rebuilt as a shear wall structure (some of the shear walls were solid steel) and it experienced heavy shaking in the 1994 Northridge earthquake. In this case, though there was no structural damage because of the very high yield strength of the building.

Figure 6.3 shows an example of a Japanese concrete shear-wall apartment building after the 1964 M 7.5 Niigata earthquake (see the figure caption).

### **Moment Resisting Frame (MRF) Buildings**

This is a very common class of buildings, whose structural system generally consists of a rectangular lattice-work of columns and beams (the frame), together with the relatively rigid floor slabs. The columns and beams can be either mild steel (SMRF) or reinforced concrete. Figure 6.4 shows an example of a SMRF. These buildings are currently popular with many architects since they are inexpensive, Office space can be easily reconfigured, and they can be quite tall (The Library Towers in downtown Los Angeles is 80 stories high).



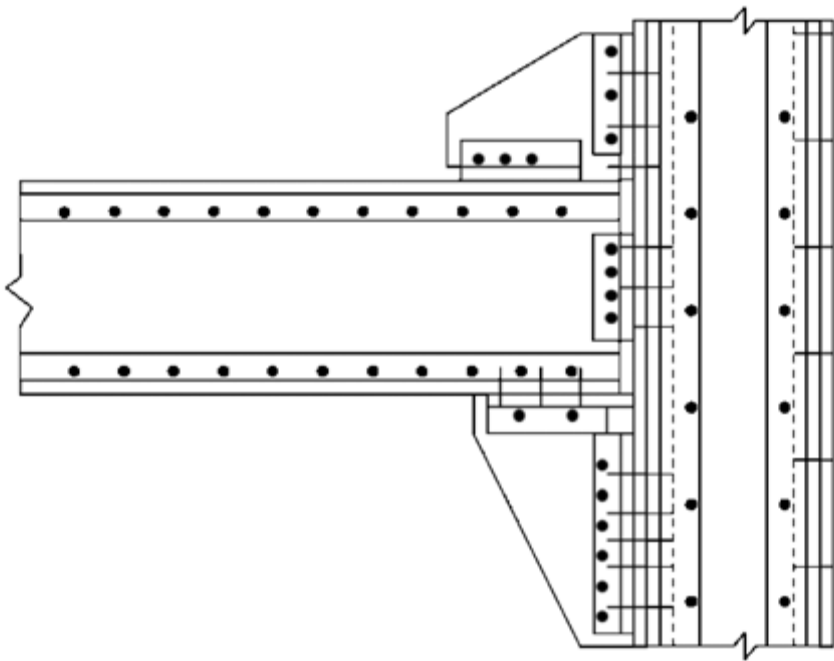
Figure 6.2 Two versions of the Olive View Hospital in the San Fernando Valley. The top picture shows the heavy damage that occurred to the first hospital (non-ductile concrete) in the 1971 M 6.7 San Fernando earthquake. The bottom picture shows the shear-wall structure that replaced the first one. This strong building had no structural damage as the result of the violent shaking in the 1994 M 6.7 Northridge earthquake.



Figure 6.3. Japanese concrete shear-wall apartment buildings after the 1964 M 7.2 Niigata earthquake. Despite the fact that the foundations of the buildings failed due to liquefaction, the building structures were undamaged and the buildings were later jacked back to an upright position and they were reoccupied.



The Home Insurance Building – Chicago, IL, 1885,  
an early skyscraper



Typical early moment connection, consisting of heavy triangular gusset plates, angles, and rivets connecting built-up columns and beams.



Steel frame buildings in downtown San Francisco performed well in the 1906 earthquake.

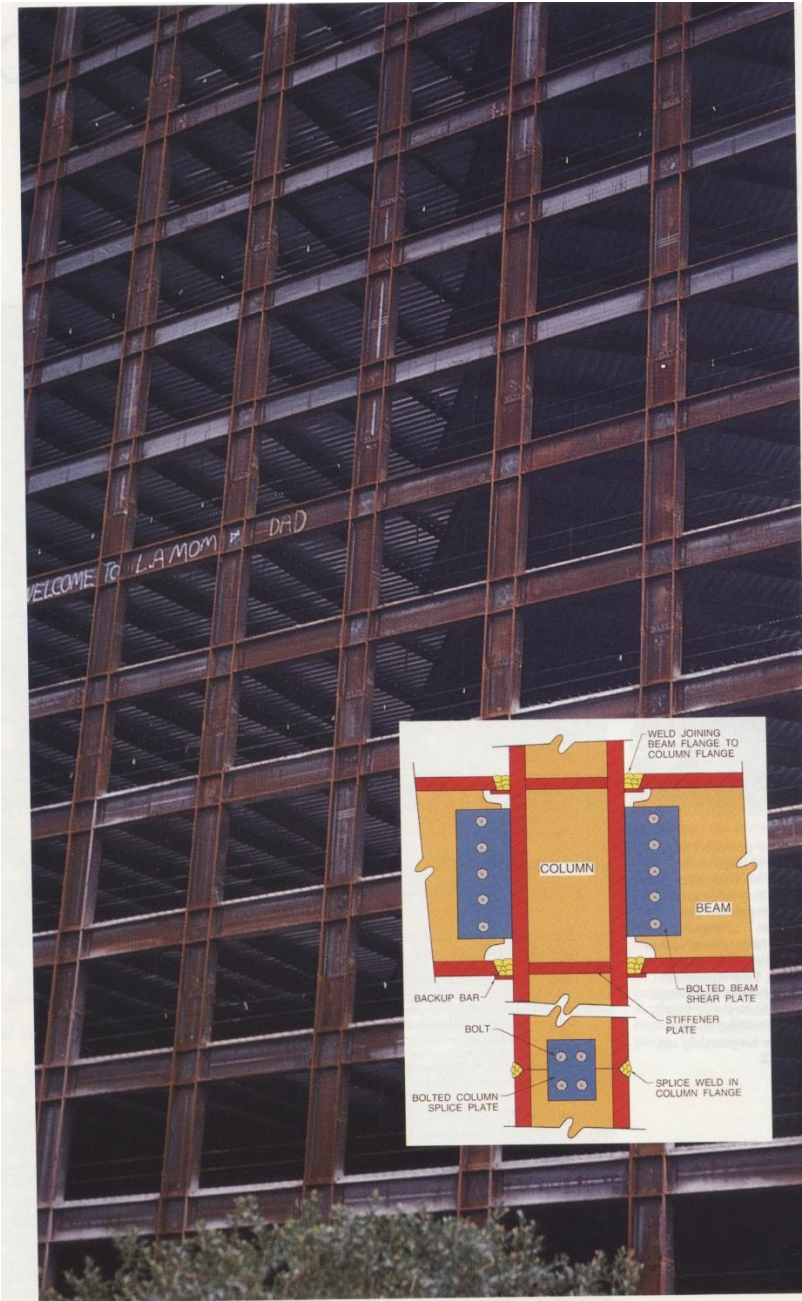
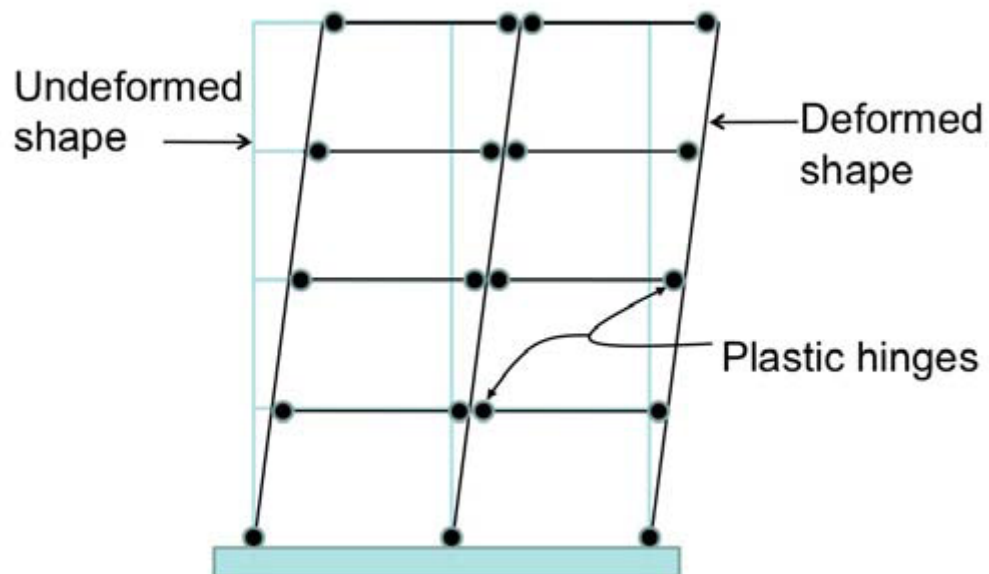


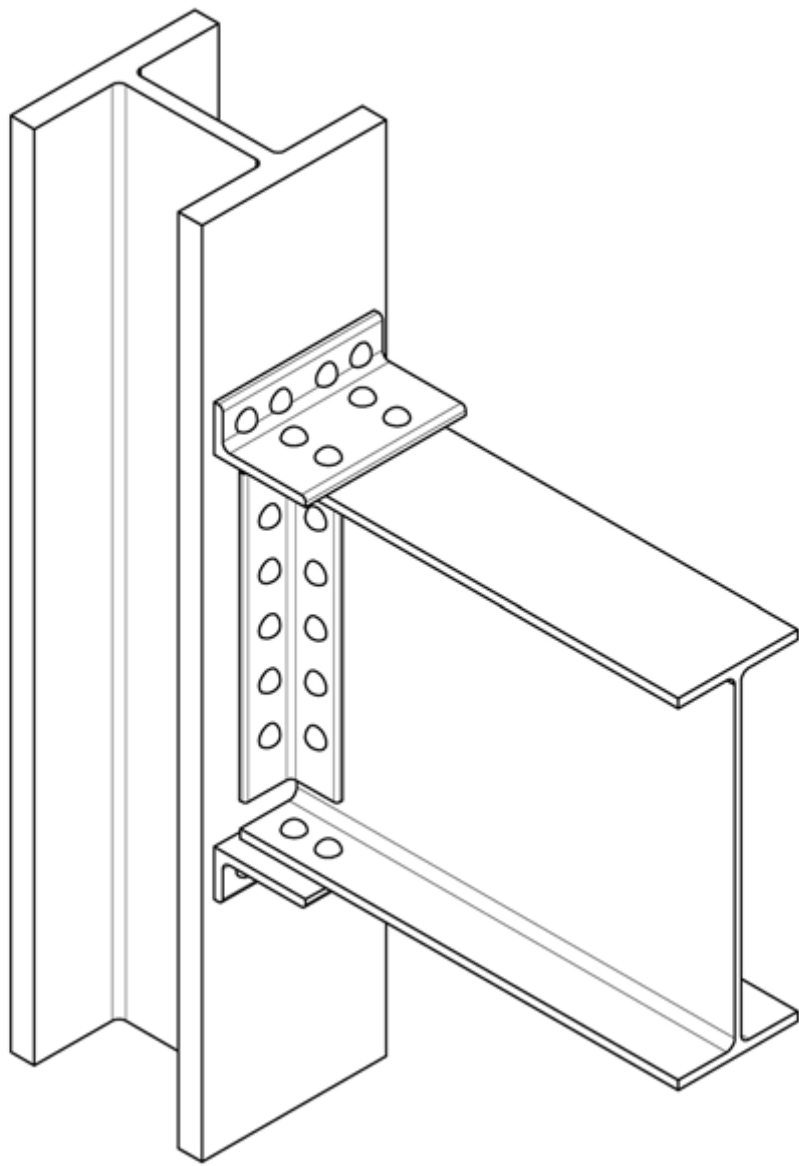
Figure 6.4. Example of a steel moment resisting frame. The connections between the beams and columns are typically welded (called a moment-resisting connection) to keep the elements perpendicular. Many of these critical connections were observed to fracture in the 1994 Northridge earthquake.



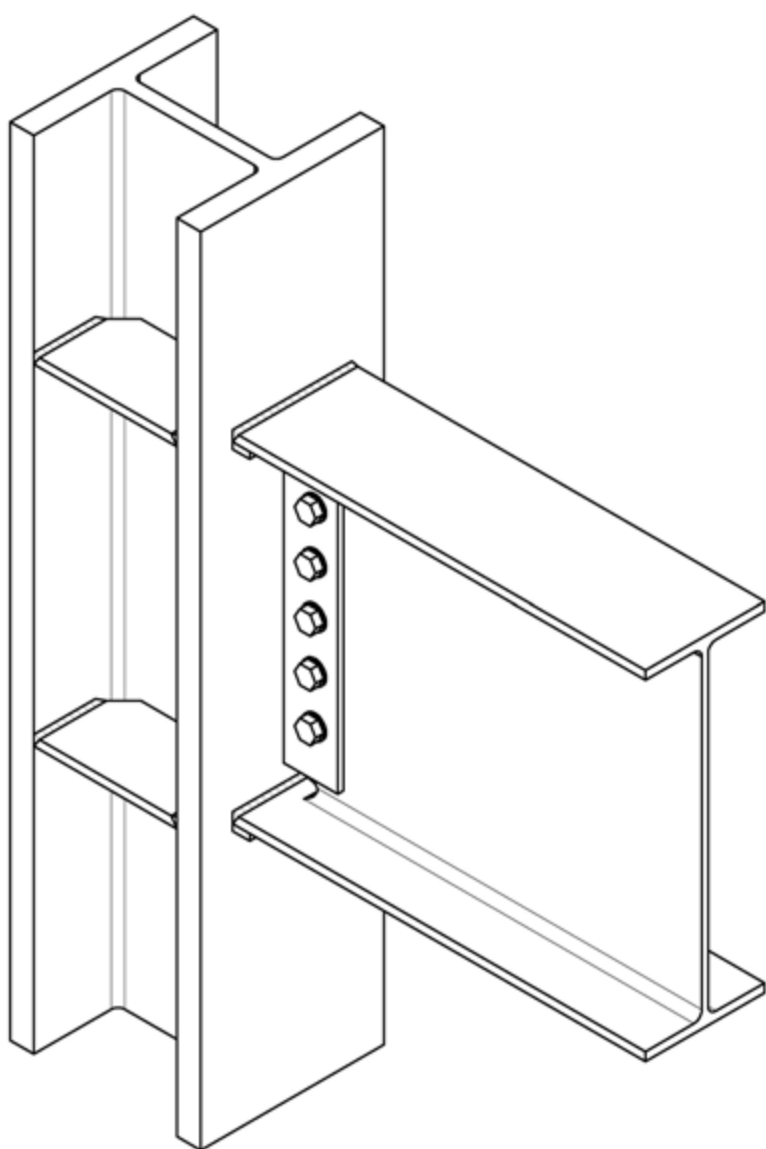
Fracturing of W14 column at welded beam-to column connection in Northridge earthquake.



Idealized sidesway mechanism intended for columns with strong-column / weak-beam design.



Riveted, unstiffened seat angle connection



Welded unreinforced flange – bolted web connection popularly used in the era 1970-1994



Post Northridge Special Moment Resisting connection (welded and bolted) in one direction and simple connection in the orthogonal direction

Figure 6.5 shows the basic physics of how an MRF resists lateral motion. As the frame is deflected horizontally, the beams and columns must bend if their connections remain perpendicular. Note that only the interior connections are moment resisting, while the exterior connection is a simple connection, which acts structurally more like a hinge. These beam-column connections are critical elements of a MRF since that is where the bending moment originates on a beam or column. It is critical that the MRF failure strength exceeds the flexural yield strength of the beams, since a building's ductility (high ductility is good) derives from the inelastic bending of beams (it's not good to inelastically bend columns since they carry gravitational loads).

In the case of Steel MRF's, the moment resisting column-beam connections typically consists of welds between the flanges of the beams and columns (see Figure 6.4). These welded connections became popular in the 1960's since they are inexpensive to use, and they were thought to have high strength. However, many of these welded connections fractured during the 1994 M 6.7 Northridge earthquake, so many of the existing steel MRF's are not as ductile as designers thought when buildings were constructed.

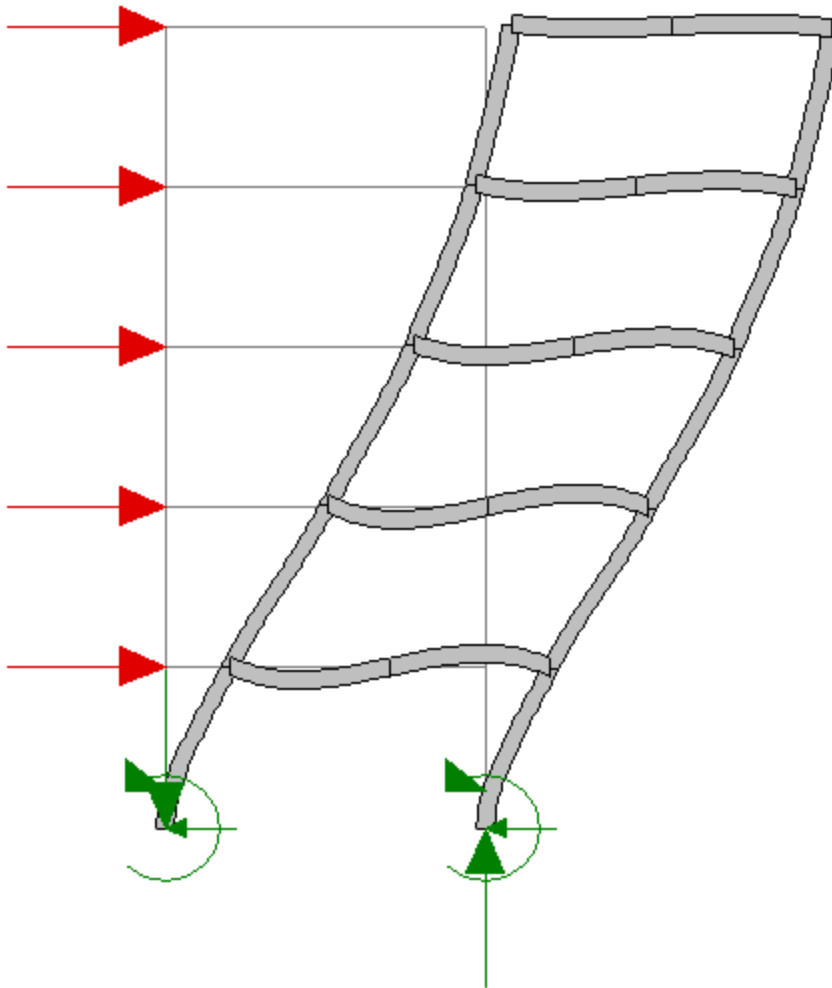


Figure 6.5. Cartoon showing how the flexural bending of beams and columns provides a resistance to lateral deformation for a moment-resisting frame structure. Note that only the connections on the exterior are moment frame connections, whereas the interior connection is a “simple” connection (unwelded) that acts more like a structural hinge.

While steel MRF's have the advantage that they are very flexible, that comes with the penalty that they have very low lateral strength. Figure 6.6 shows a **pushover analysis** (finite-element analysis by John Hall) of 20-story SMRF building that meets the 1992 UBC code for California. This analysis included numerous nonlinear effects on the deformation of the steel, as well as also explicitly including the effect of how gravitational forces act on the building for large finite displacements. That is, when the drift of the building becomes large, then every increasing lateral loads are put on the building by gravity (kind of like the Tower of Pisa). This is known as the  $P-\Delta$  effect and it is an important collapse mechanism for buildings.

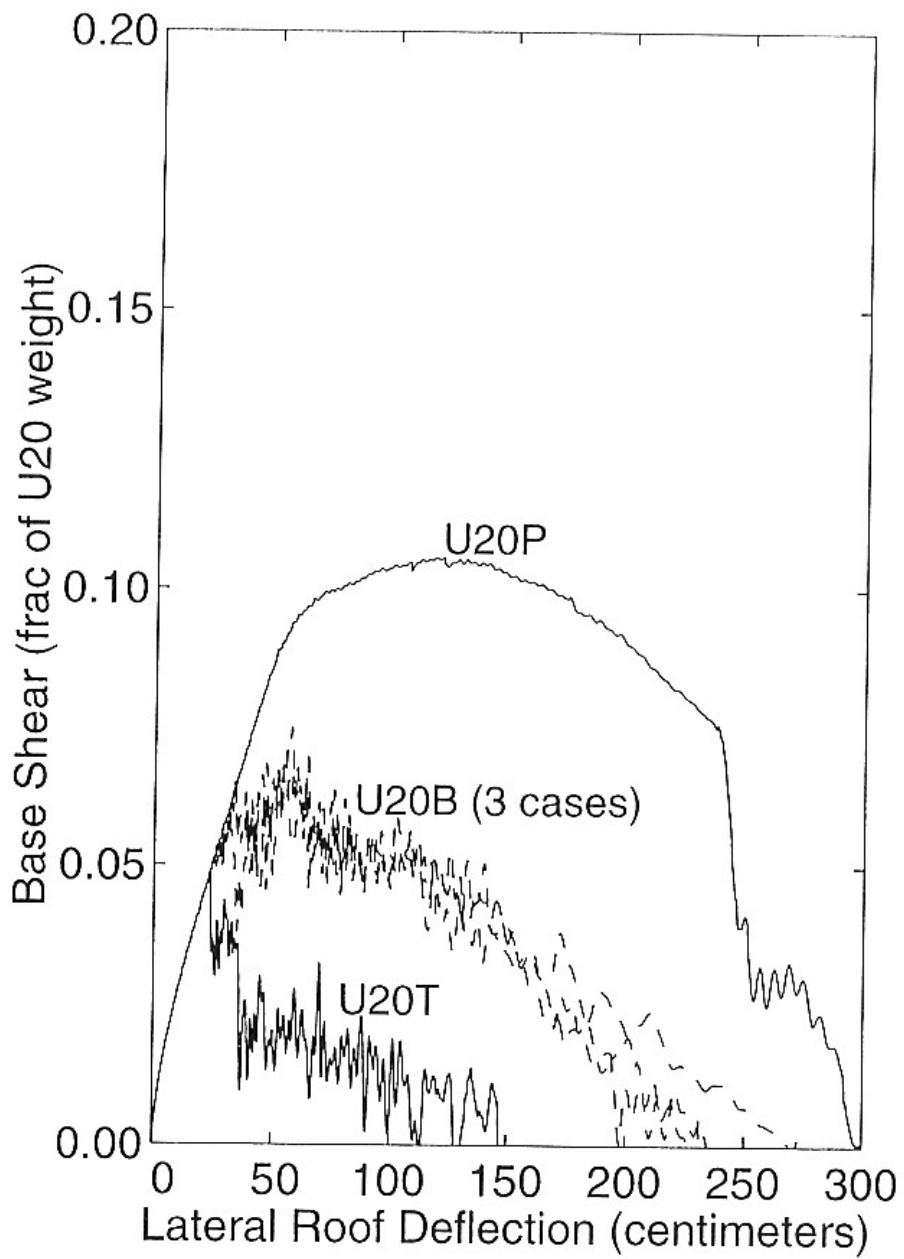


Figure 2.7 Push-over results for U20.

Figure 6.6 (from John Hall). Finite-element pushover analysis of a 20-story building that meets the 1992 US code standards for zone 4. P refers to the assumption that the moment frame connections do not fracture, B assumes that weld fractures occur randomly at stresses compatible with what was observed in the Northridge earthquake, and T assumes that the welds had even less fracture resistance.

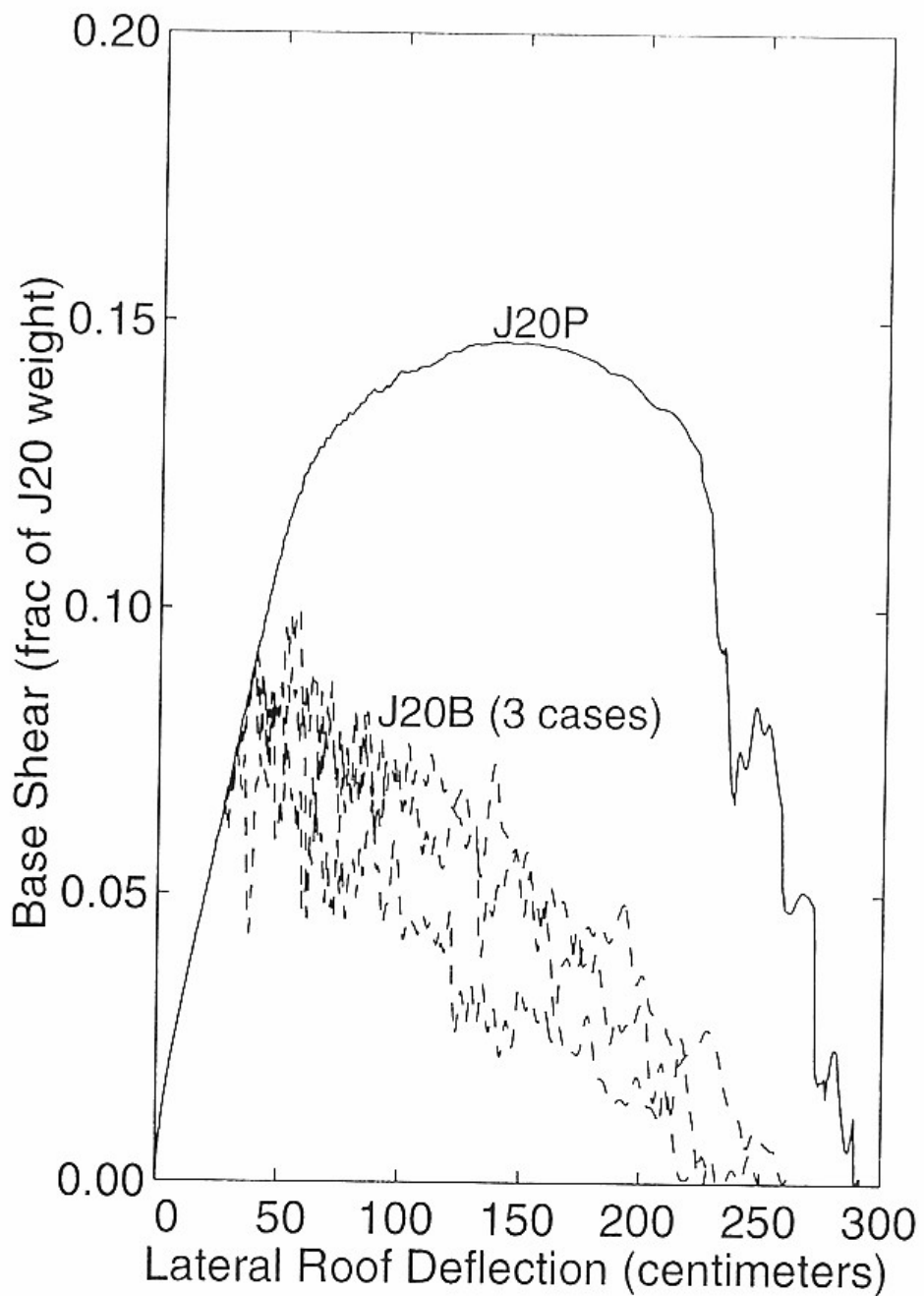


Figure 2.8 Push-over results for J20.

Figure 6.7. (from John Hall) Same as Figure 6.6., except for a 20 story steel fram building that meets Japanese codes in place in the 1990's. Notice the higher yield strength compared to the US building.

The curves U20P refer to a 20 story building that meets US 1992 zone 4 codes, and for which the welded moment resisting connections behave perfectly (no failures). The curve that is designated as B refers to allowing failure of the moment resisting connections assuming weld behavior consistent with observations in the 1994 Northridge earthquake. T refers to the assumption of terrible performance of the welds. Notice that weld failure significantly decreases both the yield strength and the ductility of the structure. Also notice that a horizontal force of only 7% of the weight of the building is necessary to push over a typical 20-story building in high seismic risk areas of the US.

Figure 6.7 shows a similar analysis, but it assumes that the building meets the building code in force in Japan in the 1990's. Japanese construction tends to put more emphasis on the yield strength of a structure, and it is common that all connections in a Japanese structure are moment-resisting connection (more costly than the US).

As it turns out, the code required yield strength tends to increase as building height both increases and decreases from 20 stories. This is because design forces for wind loads increase as the building becomes taller, whereas design forces for earthquakes decrease as the building becomes taller (we'll visit this later). So buildings shorter than 20 stories are designed for earthquake loads and buildings taller than 20 stories are designed for wind loads.

Figures 6.8 and 6.9 show the pushover analyses of 6-story steel moment resisting frame buildings for 1990's US and Japanese codes, respectively. Notice that the 6-story buildings are required to have a greater yield strength than the 20 story buildings.

Moment resisting frame buildings can also be constructed with reinforced concrete beams and columns. Concrete mrf's have similar flexibility to steel mrf's and the code requirement for pushover yield strength is also similar. Both types of mrf's are required to have high ductility (approximately a factor of 10), but this is achieved in different ways with concrete. While steel is naturally ductile in tensional strain, unreinforced concrete is naturally brittle in tension (it is very strong in compression however). Steel reinforcing bars (rebar) are run longitudinally in concrete beams in order to greatly increase the tensional strength and ductility. While longitudinal rebar is very important, it is not sufficient to make a beam adequately ductile. This was discovered through the inspection of elements that failed in shear deformation in the 1971 San Fernando earthquake. An example of this type of failure is seen in Figure 6.10, which shows the failure of a freeway bridge column during the 1994 Northridge earthquake. Notice that the column originally fractured because of horizontal shear loads on the column. Once the concrete in the column cracked, the concrete fell away from the column and the remaining rebar buckled into a mushroom shape. This is an example of **non-ductile concrete** behavior. This deficiency was rectified by requiring spiral reinforcing bars that serves to confine the concrete to the beam, even if it is fracture. Figure 6.11 shows how a concrete column can continue to carry significant loads even though it has been strained well beyond its yield point. Unfortunately, this parking garage suffered significant collapse because the elements of the building were insufficiently connected to each other. That is, the reinforcing bars must adequately tie the different elements together.

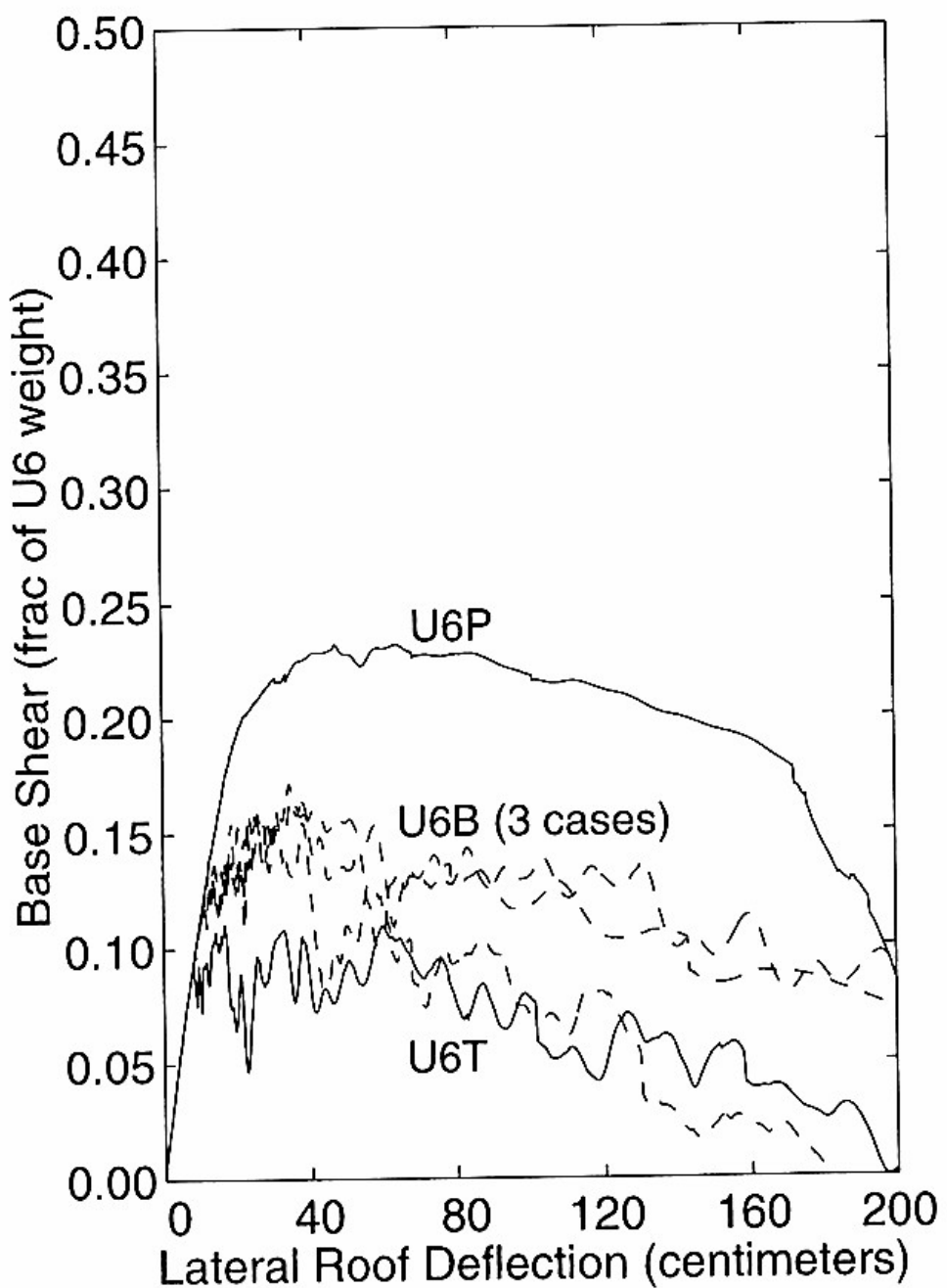


Figure 2.5 Push-over results for U6.

Figure 6.8 from John Hall. Same as Figure 6.6, but for US code 6-story steel frame building.

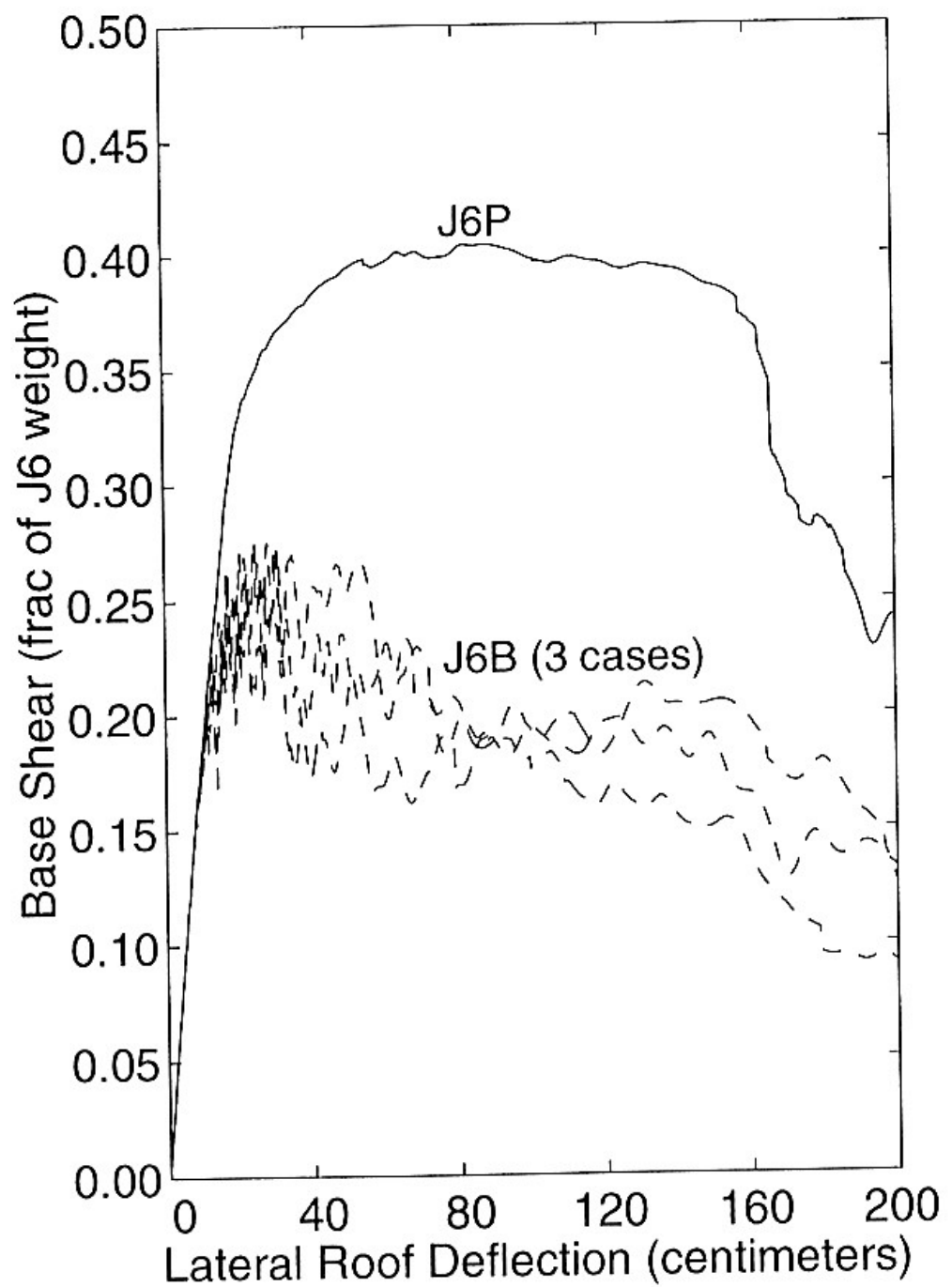
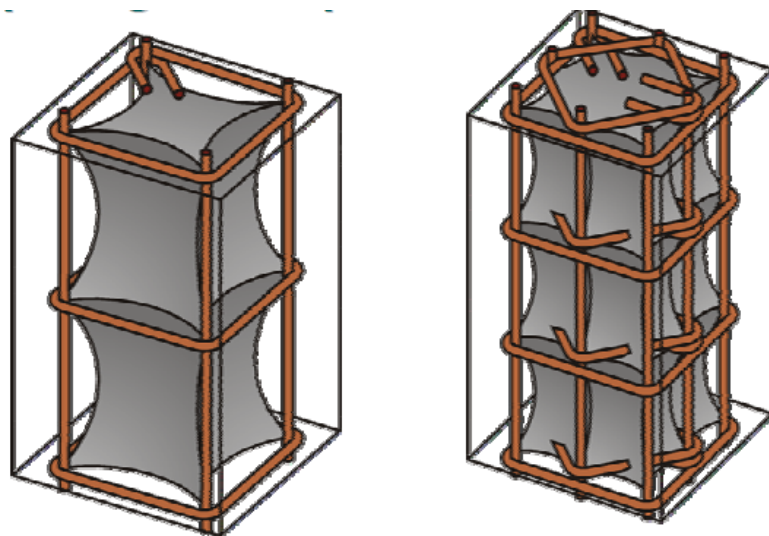


Figure 2.6 Push-over results for J6.

Figure 6.9 from John Hall. Same as Figure 6.6, but for Japanese code 6-story steel frame building



Figure 6.10. Example of a nonductile concrete column failure on a freeway bridge during the 1994 Northridge earthquake. The column was fractured by horizontal shear, the concrete fell away, and then the weight of the bridge deck caused the rebar to buckle. This failure could have been avoided by adding more spiral reinforcing loops radially around the column to make it more ductile.



Effect of confinement on the capacity of reinforced concrete

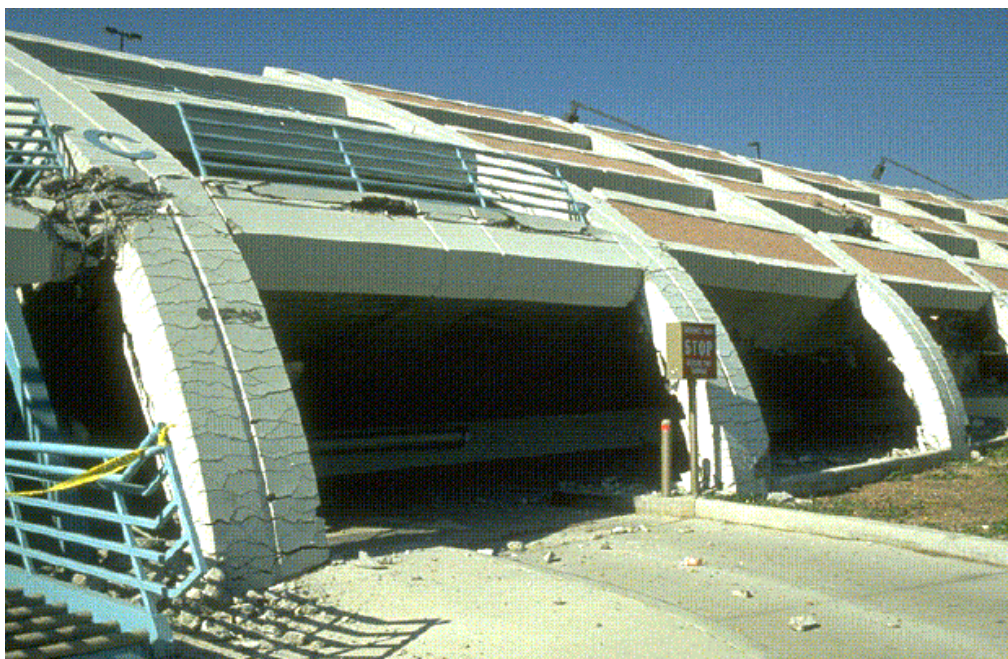


Figure 6.11. Example of ductile deformation of concrete columns from the 1994 Northridge earthquake. Adequate spiral reinforcing resulted in more ductile behavior than was shown in Figure 6.10. Unfortunately the structure had other inadequacies that led to collapse as is shown in Figure 6.12.



Figure 6.12. Despite the ductile behavior of the concrete columns, this parking structure collapsed because the floor slabs were not adequately connected to the rest of the

structure. That is, the beams and columns were ductile, but the connections between these elements were not.

Non-ductile concrete frame buildings are recognized as a class of particularly dangerous structures. They have the particularly bad combination of having a low yield stress combined with a low ductility (they're brittle). The tremendous loss of life in the 1999 Izmet Turkey earthquake was an example on non-ductile concrete frame failure. These failures are often very disastrous since the building often pancakes into a pile of floor slabs (very nasty). Figure 6.13 shows an example of the remains of an 8-story non-ductile concrete frame building that collapse in Mexico City in the 1957 Acapulco earthquake. Many concrete moment resisting frame buildings that were constructed in the United States prior to 1975 can also be classified as non-ductile concrete frames. Failures in the 1971 San Fernando earthquake resulted in a building code change in 1975 that significantly enhanced the ductility of buildings built after 1975. Unfortunately, there are no ordinances that force a building owner to strengthen these buildings. Furthermore, most of the occupants of these buildings are not aware of the potential deficiencies of their building.



Figure 6.13. Collapse of an 8-story non-ductile concrete moment resisting frame building in Mexico City from the 1957 Acapulco earthquake.

### Braced Frame Structures

The lateral yield strength of a building can be increased by adding diagonal braces to a structure, as is shown in Figure 6.13. While diagonal braces increase the yield strength, they also increase the stiffness of a building. That is, there is a trade-off between the

desired trait of high strength and the undesired trait of high stiffness. Furthermore, it can be difficult to make a braced frame that has high ductility. This is because the use of large bracing elements tends to result in very stiff braces that apply very large loads to their connections with the structure, thereby concentrating damage at these connections. However, the use of small diameter bracing elements can end up with braces that tend to have ductile extension, but they buckle in compression. As a building undergoes cyclic loading, small braces become ineffectual, since they permanently extend and buckle (see Figure 6.14). Caltech's Broad Center is one of the first buildings in the United States to use new style of brace called an unbonded brace. This consists of a small diameter steel brace that is jacketed in a concrete liner. There is a lubricating element between the concrete and the steel. The concrete jacket prevents the brace from buckling in compression and hence this brace is ductile in both extension and compression. Figure 6.15 shows an example of Broad Center's unbonded brace.

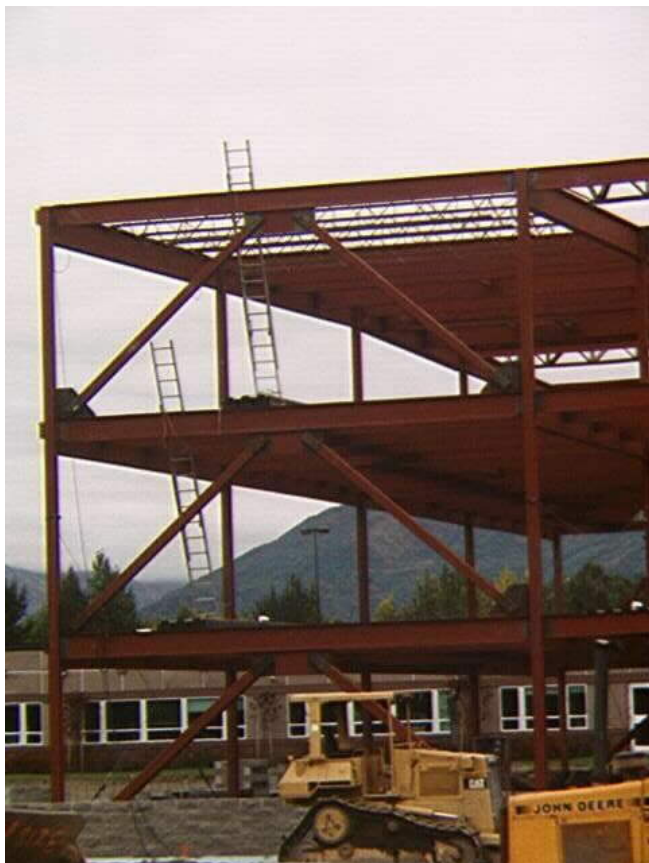


Figure 6.13. Example of a braced steel-frame.



Figure 6.15 Large braces are stiff and they put large loads into a frame, but small braces can buckle in compression.



Unbonded Brace in the Broad Center

Figure 6.14. Broad Center unbonded brace. The steel is ductile in tension and compression since it is jacketed by concrete (yellow) to prevent buckling in compression.

## Wood-Frame Structures

Wood frame is the most common type of construction in California; most residences and many commercial structures are in this category. Since wood is thought of as a “flexible” material, you might think of a very flexible building when you think of a wood frame structure. This would be a mistake. In fact, most wood frame construction is extensively braced. Furthermore, continuous plywood panels, and sheetrock panels are typically

fastened to either side of the wooden framing. Such walls may be best described as shear panels. These panels are geometrically connected into rectangular box shapes. In this sense, most wood frame construction might be better described as a shell type of structure. Another feature of wood frame construction is that the structure is relatively light (the dead load) compared with the weight of the contents (the dead load). Since it is not feasible to allow the structure to deform significantly because of the live loads (the plaster would crack), wood frame structures tend to be extremely strong (and stiff) compared to their weight. They are also relatively ductile (the framing is redundant, and nails must be pulled out to disconnect elements). As a result of these features, wood frame structures tend to perform very well in earthquakes. Despite the fact that these structures have been located in areas of violent shaking in past earthquakes, collapse of these structures is exceedingly rare. Figure 6.15 shows the Turnagain Heights housing development (wood frame) following the 1964 Alaskan Earthquake. Despite the tremendous damage caused by a massive landslide beneath the development, the wood frame houses essentially remained intact.

### 1964 Alaska Earthquake, Turnagain Heights



Figure 6.15. Wood frame houses that rode through the massive landslide triggered by the 1964 Alaskan earthquake.

## Unreinforced Masonry

In the earlier part of the 20<sup>th</sup> Century, many buildings were constructed of unreinforced brick; that is the exterior walls are several courses of brick and mortar, whereas the inner walls, floors, and roof are wood frame construction. The exterior brick walls in this type of construction tend to be heavy and brittle. That is, the walls cannot sustain tension. URM's have the undesirable characteristics that they are heavy, stiff, and quite brittle. The inadequacies of unreinforced masonry (URM) became obvious in the 1933 Long Beach earthquake and many municipalities adopted building codes (between the mid 1930's and 1950, depending on the city) that required that these masonry construction buildings should be reinforced with steel. However, several cities have numerous examples of these historic structures. Following serious damage to URM's in the 1971 San Fernando earthquake, the cities of Los Angeles and Long Beach adopted controversial legislation that required that all URM should have some strengthening. At a minimum, this involved making stronger connections between the wooden floor trusses and the brick walls. This tends to decrease the bending moments on the base of the brick walls for out-of-plane shaking. Some buildings are also reinforced by building another structural system (often steel) within the building. Although strengthened URM are an improvement on the pre-existing structures, there is a widely held belief that they are still lacking in strength and ductility. Despite their obvious shortcoming, the interior walls of URM's often prevent the catastrophic pancaking of the floors seen in non-ductile concrete frame buildings.

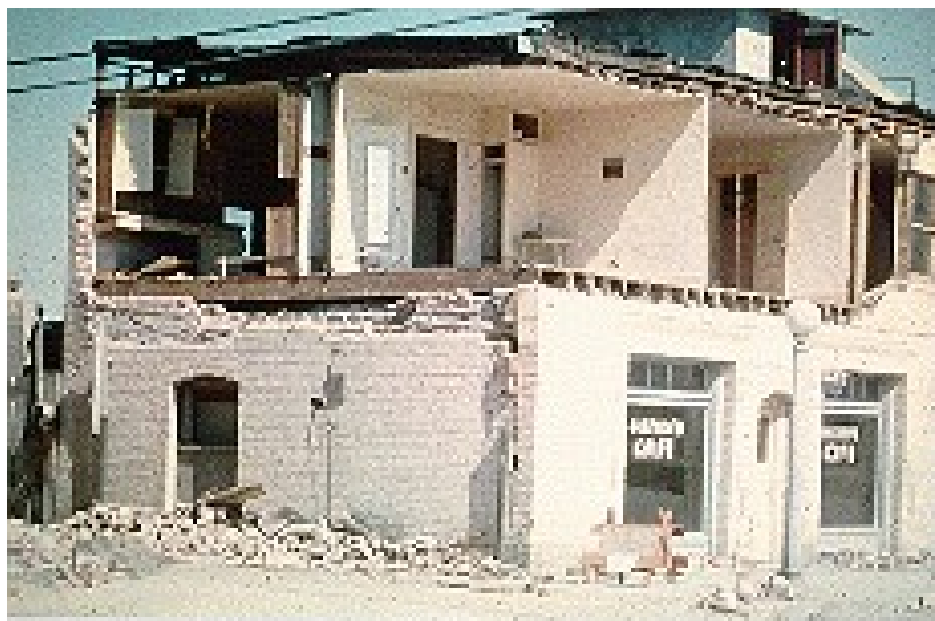


Figure 6.16. Example of an unreinforced masonry building (URM).

Table 6.1 Qualitative summary of the characteristics of different building types.

Building type	stiffness	density	yield strength	ductility
---------------	-----------	---------	----------------	-----------

Shear wall	high	high	high	medium
MRF	low	low	low	high
Braced MRF	medium	low	medium	high/medium
Wooden house	high	low	high	high
Nonductile concrete	medium	medium	low	low
URM	high	high	medium	low

## Building as a Rigid Block

Buildings are not rigid blocks! However, it is still instructive to investigate the forces in a rigid block that is subject to ground acceleration. This example has some application if the lowest natural frequency of the structure is high compared to the predominant frequency of the ground acceleration.

If both the building and the ground are considered to be rigid (how do you have earthquakes in a rigid earth?), then there are no waves and the problem can be solved by balancing force as follows. Consider a rigid building of height  $h$ , length and width  $w$ , and average density  $\rho$  be subjected to a horizontal acceleration  $\ddot{u}(t)$  as shown in Figure 6.17.

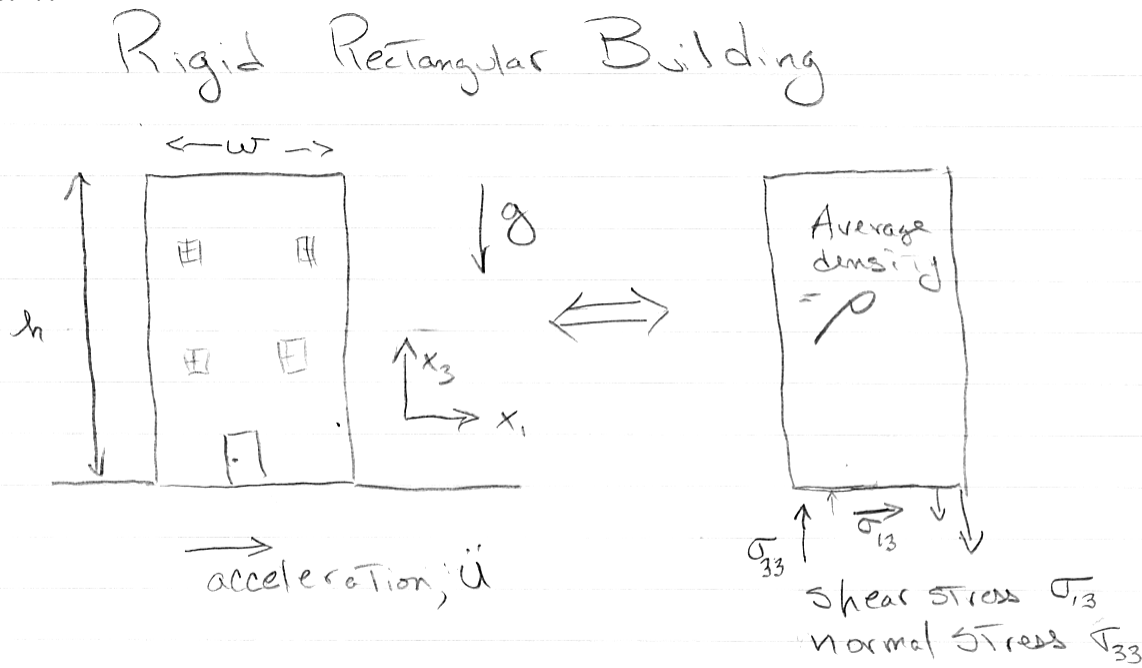


Figure 6.17. Forces acting on a rigid rectangular building that is sitting on a rigid earth. There are both shear stresses to horizontally accelerate the building, and also a moment that is applied to the base to keep the building from rotating.

The total momentum of the building can be considered to be the sum of the translation of the center of mass of the building and also the rotational momentum of the building about an axis running through the center of the building. Since the ground is considered as rigid, the building cannot rotate and the translational momentum of the building is just

$$P_1(t) = \rho h w^2 \dot{u}(t) \quad (6.1)$$

where  $P_1(t)$  is the momentum in the  $x_1$  direction (that's all there is in this problem). The total horizontal force on the bottom of the building is

$$F_1(t) = \dot{P}_1(t) = \rho h w^2 \ddot{u}(t) \quad (6.2)$$

Therefore the shear stress on the bottom of the building is just the force divided by the cross sectional area, or

$$\sigma_{13}(t) = \rho h \ddot{u}(t) \quad (6.3)$$

So the shear stress at the bottom of a rigid building on a rigid earth just depends on the ground acceleration and the height of the building (assuming that the density is constant). However, there is more to this simple problem. The shear stress at the bottom of the building would cause the building to rotate if there were no counteracting forces on the base of the building. That is the total moment applied to the base of the building must be zero, or

$$F_1(t) \frac{h}{2} - w \int_{-\frac{w}{2}}^{\frac{w}{2}} [\sigma_{33}(t, x_1) - \rho g h] x_1 dx_1 = 0 \quad (6.4)$$

where we assumed that the normal force on the base of the building consists of the weight of the building **plus** a moment that keeps the building from rotating. If we assume that the normal stress consists of constant compressional stress from the weight of the building ( $\rho g h$ ) plus another stress that varies linearly with distance along the base then

$$\sigma_{33}(x_1, t) = c(t) x_1 + \rho g h \quad -w < x_1 < w \quad (6.5)$$

where  $c(t)$  is now only a function of time. In this case

$$F_1(t) \frac{h}{2} - w c(t) \int_{-\frac{w}{2}}^{\frac{w}{2}} x_1^2 dx_1 = 0 \quad (6.6)$$

Substituting (6.2) into (6.6) and performing the integration yields

$$\frac{\rho h^2 w^2 \ddot{u}(t)}{2} - \frac{w^4}{12} c(t) = 0 \quad (6.7)$$

or

$$\sigma_{33}(x_1, t) = \rho g h + 6\rho \left( \frac{h}{w} \right)^2 x_1 \ddot{u}(t) \quad -w < x_1 < w \quad (6.8)$$

Therefore the normal stresses at the outer edges of the building are

$$\begin{aligned} \sigma_{33}(x_1 = \pm w, t) &= \rho g h \pm 3\rho \left( \frac{h}{w} \right)^2 w \ddot{u}(t) \\ &= \rho h \left[ g \pm 3 \left( \frac{h}{w} \right) \ddot{u}(t) \right] \end{aligned} \quad (6.9)$$

There are cases where engineering materials fail easily in tension. Tensional stresses in our rigid building occur at the outer edge when

$$\ddot{u} > g \frac{w}{3h} \quad (6.10)$$

Therefore, rigid buildings that are tall compared with their width can result in tensional stresses in the exterior part of the building.

If we can approximately model the dynamics of a building with a rigid block, then the stresses in the building are determined by the **peak acceleration**. However, it has been long known that the peak accelerations observed in earthquakes are considerably larger than the nominal lateral strength of buildings that have survived those ground accelerations. As it turns out, the peak acceleration in most seismic records is strongly dependent on high-frequency parts of the motion (typically  $> 3$  Hz), and the assumption that the building's fundamental frequencies are large compared to the ground acceleration does not apply.

### Rigid Building on a Flexible Foundation (Rocking)

In this section we investigate what happens if we allow a rigid building to tilt due to flexibility of the foundation. This is not a very realistic problem to consider the ground to be far more flexible than the building, but it does illustrate how forces in the base of a building can be modified by the elasticity of the soil. This is called a **soil-structure interaction** (there are other effects that enter into this problem, but this is probably the most important). The problem is sketched in Figure 6.18. However, for the current discussion, we only ask the simpler question of how the rotation of the building changes the forces on the base of the building as compared with the previous section of this chapter.

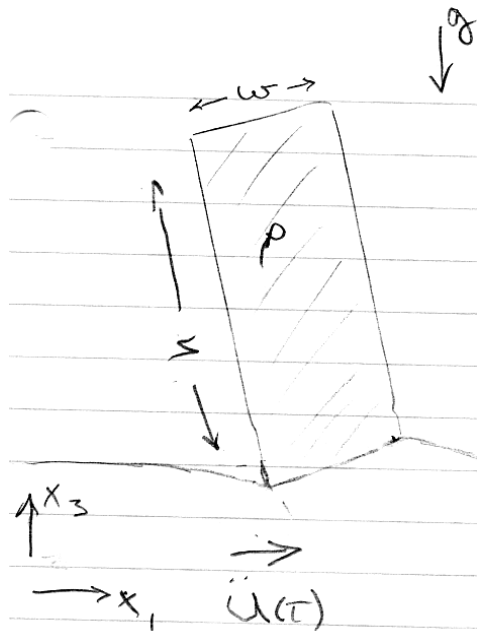


Figure 6.18 Cartoon of a rigid building on a flexible foundation

Solving for the forces in this problem involves separating the motion of the building into two parts; 1) the rectilinear motion of the center of mass of the building, and 2) the rotational motion about its axis of angular momentum. This decomposition is shown in Figure 6.19.

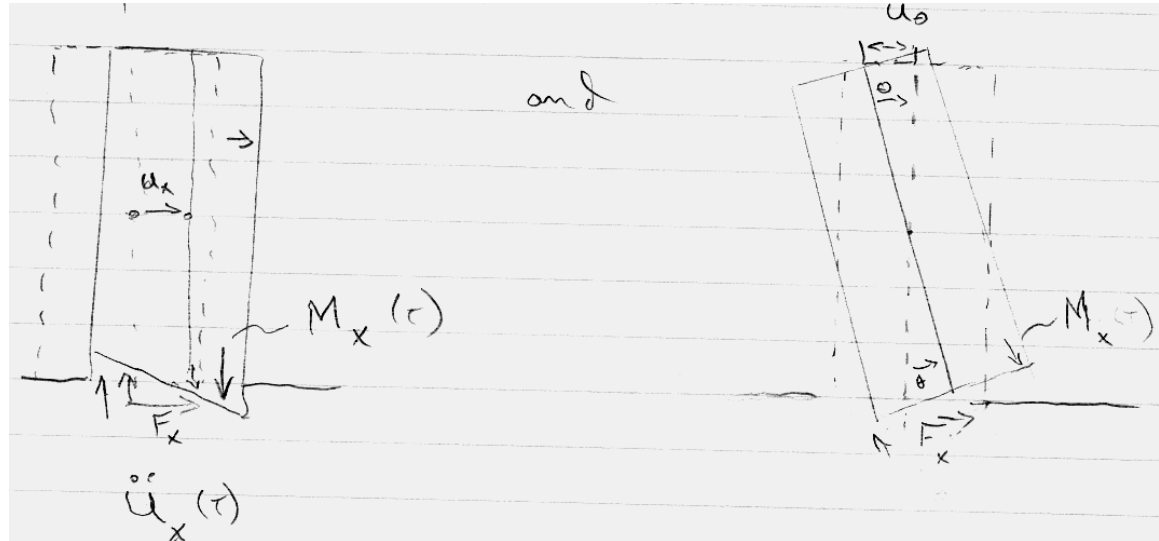


Figure 6.19 The motion of a rigid building can be viewed as the sum of a translation of the center of mass together with a rotation about the principal axis of inertia.

Let  $u(t)$  be the motion of the base of the building in an inertial frame,  $u_x(t)$  be the linear motion of the center of mass, and  $u_\theta(t)$  be the motion of the base due to pure rotation of the building about the center of rotation which is located at the midpoint of the building. Then

$$u(t) = u_x(t) + u_\theta(t) \quad (6.11)$$

and

$$\ddot{u}(t) = \ddot{u}_x(t) + \ddot{u}_\theta(t) \quad (6.12)$$

now

$$u_\theta(t) = \frac{h}{2} \sin \theta(t) \approx \frac{h}{2} \theta(t) \quad \theta \ll \pi \quad (6.13)$$

then

$$\ddot{u}_\theta(t) \approx \frac{h}{2} \ddot{\theta}(t) \quad (6.14)$$

The force system on the base of the building can be considered to be the sum of the a horizontal force  $F_1(t)$  (these are unbalanced) and a resisting moment  $M(t)$  caused by the distribution of vertical stresses on the base of the building. The rectilinear momentum of the building  $P(t)$  is just

$$P(t) = \rho w^2 \int_0^h \left( \dot{u}(t) - \frac{1}{2} x_3 \dot{\theta}(t) \right) dx_3 = m \left( \dot{u}(t) - \frac{1}{2} h \dot{\theta}(t) \right) \quad (6.15)$$

where  $m = \rho h w^2$  is just the mass of the building. The force on the base of the building is then

$$F_1(t) = \dot{P}(t) = m \left( \dot{u}(t) - \frac{1}{2} h \dot{\theta}(t) \right) \quad (6.16)$$

The shear stress on the base of the building is then

$$\sigma_{13}(t) = \frac{F_1(t)}{w^2} = \frac{\dot{P}(t)}{w^2} = \rho h \left( \ddot{u}(t) - \frac{1}{2} h \ddot{\theta}(t) \right) \quad (6.17)$$

At this point, we do not yet know the shear stress, since we do not know  $\theta(t)$ . We can calculate the rotation of the building as follows,

$$M(t) + F_1(t) \frac{h}{2} = I \ddot{\theta}(t) \quad (6.18)$$

where

$$I = \frac{1}{12} m (h^2 + w^2) \quad (6.19)$$

Combining (6.16), (6.17), and (6.19) yields

$$\ddot{\theta}(t) = \frac{12}{m(4h^2 + w^2)} \left[ M(t) + \frac{mh}{2} \ddot{u}(t) \right] \quad (6.20)$$

Now the moment at the base of the building is

$$M(t) = w \int_{-\frac{w}{2}}^{\frac{w}{2}} \sigma_{33}(t) x_i dx_i \quad (6.21)$$

If we assume that the normal stress is proportional the vertical deflection, then

$$\sigma_{33}(t) = k \theta(t) x_i \quad -\frac{w}{2} < x_i < \frac{w}{2} \quad (6.22)$$

where  $k$  is a type of stiffness with units of stress per unit of displacement (it differs from a regular spring constant, which has units of force per unit displacement). Therefore,

$$M(t) = wk\theta(t) \int_{-\frac{w}{2}}^{\frac{w}{2}} x_i^2 dx_i = \frac{1}{12} w^4 k \theta(t) \quad (6.23)$$

Combining (6.20) and (6.23) gives us the equation for a single degree of freedom forced oscillator

$$\ddot{\theta}(t) - \frac{kw^4}{m(4h^2 + w^2)} \theta(t) = \frac{6h}{(4h^2 + w^2)} \ddot{u}(t) \quad (6.24)$$

We immediately recognize that this is an un-damped forced linear oscillator with a natural period of

$$\omega_0 = w^2 \sqrt{\frac{1}{4h^2 + w^2}} \sqrt{\frac{k}{m}} \quad (6.25)$$

The full solution to this force oscillator is given in Chapter 1 (see equation 1.40 with damping equal to zero) as

$$\theta(t) = \frac{6h}{(4h^2 + w^2)} \ddot{u}(t) * \left[ H(t) \frac{\sin \omega_0 t}{\omega_0} \right] \quad (6.26)$$

While we have modeled the building as an un-damped SDOF, the full solution to this problem is quite complex, since the oscillations of the building would excite waves in the elastic medium. The excitation of the waves would cause kinetic energy in the building to be radiated as wave energy into the surrounding medium. This would be a form of radiation damping of the oscillations of the building. Substituting (6.26) into (6.17) gives

$$\begin{aligned} \sigma_{13}(t) &= \rho h \left( \ddot{u}(t) - \frac{3h^2}{(4h^2 + w^2)} \ddot{u}(t) * \frac{\partial^2}{\partial t^2} \left[ H(t) \frac{\sin \omega_0 t}{\omega_0} \right] \right) \\ &= \rho h \ddot{u}(t) * \left( \delta(t) - \frac{3h^2}{w^2 \sqrt{4h^2 + w^2}} \sqrt{\frac{m}{k}} \frac{\partial^2}{\partial t^2} \left[ H(t) \sin \omega_0 t \right] \right) \end{aligned} \quad (6.27)$$

We can also calculate the vertical compressive stresses at the outer edges of the building by substituting (6.26) into (6.22).

$$\begin{aligned} \sigma_{33}(t; x_l = \pm w) &= \rho g h \pm k w \theta(t) \\ &= \rho g h \pm k w \frac{6h}{(4h^2 + w^2)} \ddot{u}(t) * \left[ H(t) \frac{\sin \omega_0 t}{\omega_0} \right] \\ &= \rho g h \pm \frac{6h}{w \sqrt{4h^2 + w^2}} \sqrt{mk} \ddot{u}(t) * \left[ H(t) \sin \omega_0 t \right] \end{aligned} \quad (6.28)$$

These are fairly complex relationships. However, we can get some idea of the effect of building tilting by investigating the initial response of the building to a impulse in acceleration,  $\ddot{u}_{\max}$ . In this case (6.27) becomes

$$\begin{aligned} \sigma'_{13}(t) &= \rho h \ddot{u}_{\max} \left( \delta(t) - \frac{3h^2}{(4h^2 + w^2)} \delta(t) * \frac{\partial^2}{\partial t^2} \left[ H(t) \frac{\sin \omega_0 t}{\omega_0} \right] \right) \\ &= \rho h \ddot{u}_{\max} \left( \delta(t) - \frac{3h^2}{(4h^2 + w^2)} \frac{\partial}{\partial t} \left[ \delta(t) \frac{\sin \omega_0 t}{\omega_0} + H(t) \cos \omega_0 t \right] \right) \\ &= \rho h \ddot{u}_{\max} \left( \delta(t) - \frac{3h^2}{(4h^2 + w^2)} \left[ \dot{\delta}(t) \frac{\sin \omega_0 t}{\omega_0} + 2\delta(t) \cos \omega_0 t - H(t) \omega_0 \sin \omega_0 t \right] \right) \\ &= \rho h \ddot{u}_{\max} \delta(t) \left( 1 - \frac{6h^2}{(4h^2 + w^2)} \cos \omega_0 t \right) - \rho h \ddot{u}_{\max} H(t) \omega_0 \sin \omega_0 t \end{aligned} \quad (6.29)$$

Or we can write the shear response for an arbitrary acceleration as

$$\sigma'_{13}(t) = \rho h \ddot{u}(t) \left( 1 - \frac{6h^2}{(4h^2 + w^2)} \cos \omega_0 t \right) - \rho h \ddot{u}(t) * H(t) \omega_0 \sin \omega_0 t \quad (6.30)$$

Therefore, the shear maximum shear stress is decreased for a rocking building compared with a rigid building (that is, for an impulse of acceleration). To fully understand the effect of this rocking, we would have to know the actual ground acceleration time history. If the ground motion was harmonic with the same period as the natural frequency of rocking, then the rocking building would resonate with the ground. If the duration of the ground motion was large enough, then the rocking building would develop even larger shears than the rigid building on the rigid foundation.

Notice that the acceleration impulse response for the outer edges of the building can be derived from (6.28), and is

$$\begin{aligned}\sigma_{33}(t; x_1 = \pm w) &= \rho gh \pm \frac{6h}{w\sqrt{4h^2 + w^2}} \sqrt{mk} \ddot{u}_{\max} \delta(t) * [H(t) \sin \omega_0 t] \\ &= \rho gh \pm \frac{6h}{w\sqrt{4h^2 + w^2}} \sqrt{mk} \ddot{u}(t) * [H(t) \sin \omega_0 t]\end{aligned}\quad (6.31)$$

Notice that as  $k \rightarrow 0$ , a very, very flexible foundation, then

$$\sigma_{33}(t; x_1 = \pm w) = \rho gh \quad t \ll \omega_0 \quad (6.32)$$

That is, as the foundation becomes more flexible, the normal stresses on the columns decrease. However, depending on the convolution term, there may be resonances and the compressive stresses may actually increase.

### Flexible Building as a Continuous Cantilevered Beam

The problem of the dynamic motions of a continuous prismatic beam can give us some insight into the deformation of buildings. To solve such a cantilevered beam problem in full generality is exceeding complex. To begin with we recognize that, if the building is considered as a continuum, it would often be anisotropic. For example, consider an mrf. The stiffness associated with inter-story drift ( $\varepsilon_{13}$  and  $\varepsilon_{23}$ ) would be much less than the stiffness associated with shearing the actual floor slabs  $\varepsilon_{12}$ . Likewise the stiffness associated with extension along columns ( $\varepsilon_{33}$ ) is different than for extension along the floor slabs ( $\varepsilon_{11}$  and  $\varepsilon_{22}$ ). However, we will assume that only parts of the strain tensor which are important to describe the deformation of the building are inter-story shear strain and extensional strain along the columns. We can thus approximate the building as being isotropic, since the other elastic moduli are not important. We must also recognize that the material in our imaginary continuous beam may have a very unusual Poisson's ratio. That is, the building is very stiff in compression along the columns and very flexible in inter-story shear. That is,  $\lambda \gg \mu$ . In fact, for a tall mrf (either concrete or steel), the velocity of P-waves up the building is 10 to 20 times more than the S-wave velocity.

While the complete solution for an isotropic elastic cantilevered beam is itself quite complex, there are two end-member cases where the solution is more tractable (see figure 6.20).

The first is the case in which the height of the building is large compared to the height (a tall skinny building). In this case the building deforms primarily by bending which is the term used for extensional strains in the columns (extension and compression at the opposite sides of the building). There is a well developed theory (the technical theory of bending) which allows beam problems to be solved with the assumption that the shear strains are approximately zero. This is called a **bending beam**. The stiffness of a bending beam is determined by its flexural rigidity,  $EI$ , which scales with dimension as

$$EI = \int_0^w \int_0^w x_1^2 dx_1 dx_2 = \frac{E}{3} w^4 \quad (6.33)$$

where  $E$  is the Young's modulus and the building is assumed to have a square cross section of width  $w$ . The building becomes very stiff against flexure as  $w$  becomes large.

In the second case the building is assumed to be much wider than it is tall. When the ground beneath the building moves horizontally, this is identical to the problem of having an SH wave propagate vertically in a layer of building; the bending is approximately zero in this case. This is called a **shear beam**. In this case the total stiffness against shear is just the shear modulus times the cross sectional area ( $\mu w^2$ ). Therefore, it is easy to see why a wide building is dominated by shear and not by bending.

While actual buildings are neither a true bending beam nor a shear beam, we can gain some useful insight by looking at these approximate modes of deformation.

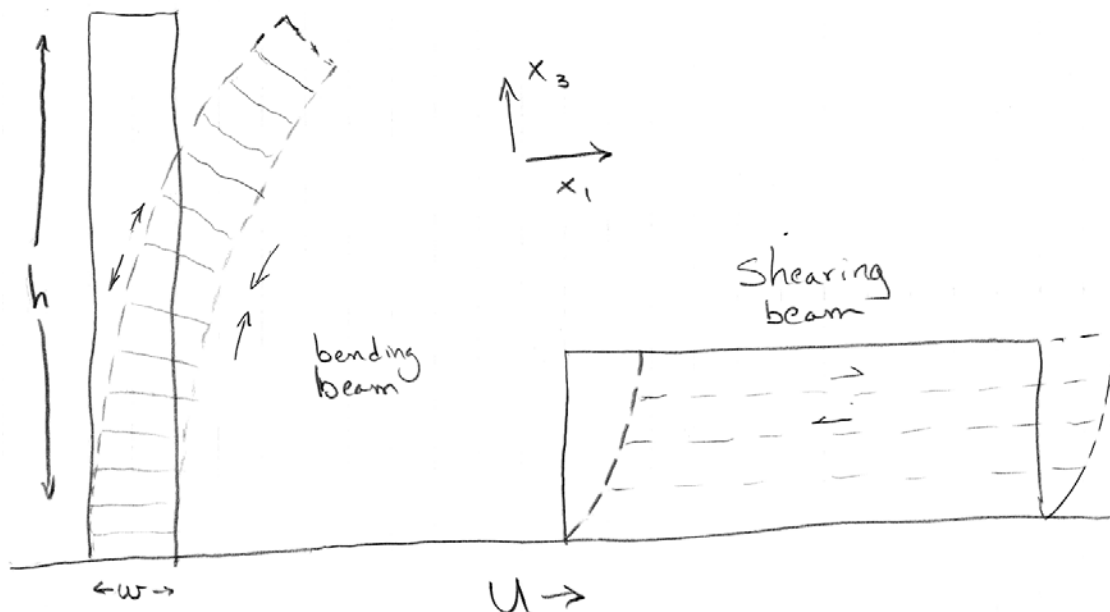


Figure 6.20. Cartoon on the left is a bending beam (negligible inter-story shear strains). Most of the deformation occurs because of compression and extension of the outer

columns. Cartoon on the right is a shearing beam (negligible extension/compression on the columns). The floor slabs remain horizontal.

### Flexible Building as a Shearing Beam

Figure 6.21 shows the horizontal accelerations that occurred on different floors of a 52-story steel mrf building in downtown Los Angeles during the 1994 Northridge earthquake. Notice the prominent pulse of acceleration that occurs at the base of the building at about 14 seconds into the record. This pulse can be observed to propagate up the building and it arrives at the top about 1.5 seconds later. Also notice that the pulse is twice as large on the roof as it is in the rest of the building. You can even see a hint that the pulse travels back down the building after it reflects off the top. This type of behavior is exactly what we expect from a shear beam. It is identical to the problem of a vertically propagating SH wave in a plate with a rigid boundary at the bottom and a free boundary at the top. We already extensively discussed this problem in Chapter 4.

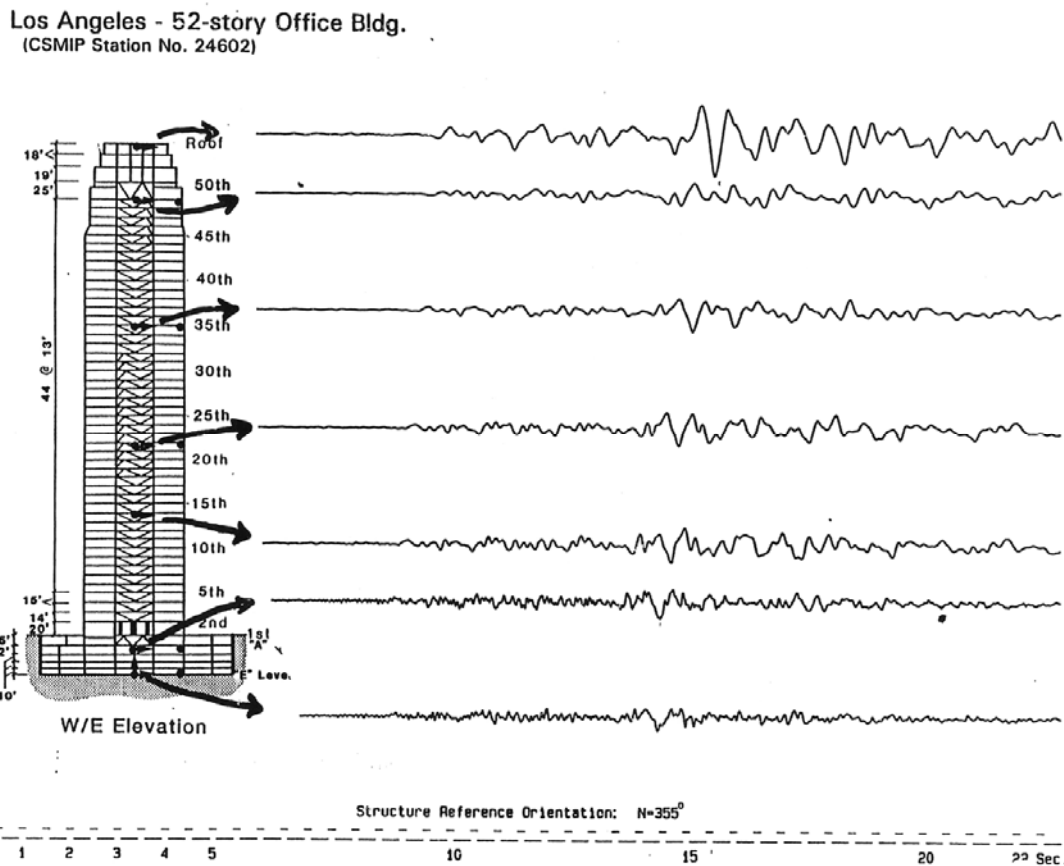
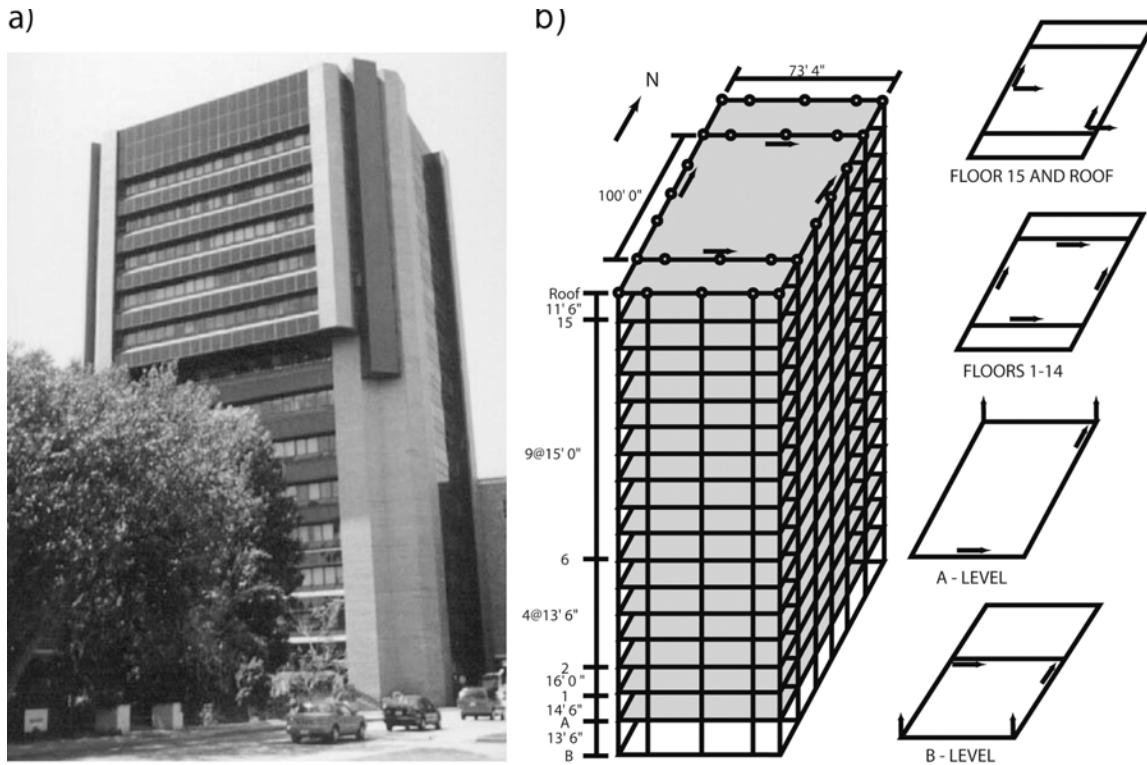
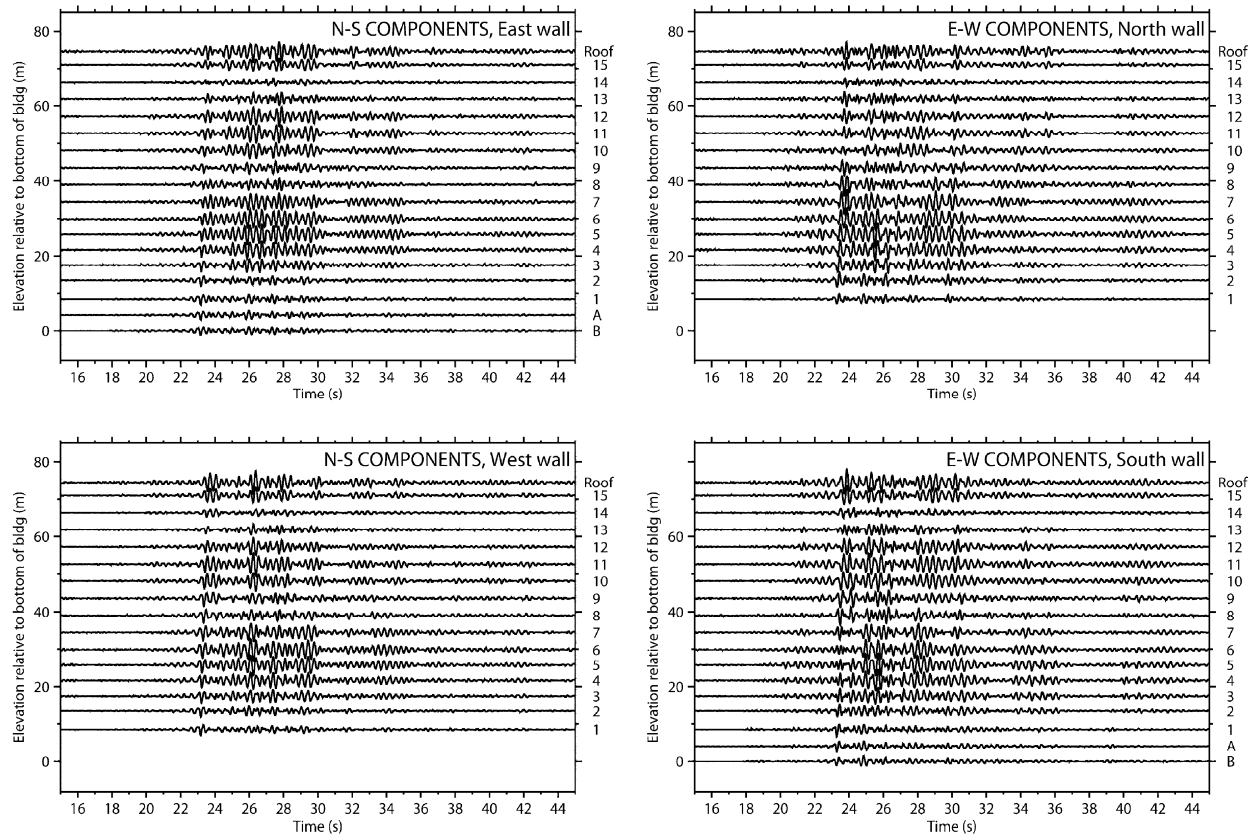


Figure 6.21. Horizontal accelerations in a steel mrf during the 1994 Northridge earthquake. Notice the vertically propagating pulse.



The Factor building (a) and its seismicarray (b). Arrows show polarities of the single component sensor.

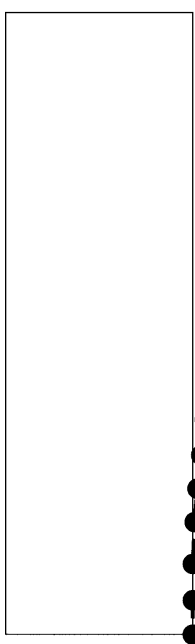


Displacement records for the 16 December 2004 Santa Monica Bay ( $M_{\text{L}} 3.6$ ) earthquake. The figure shows the north-south components for sensors on the

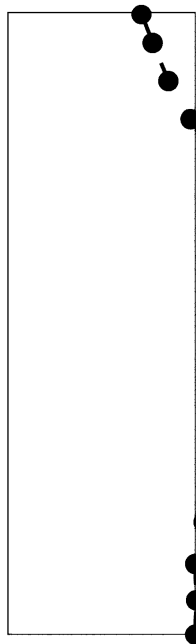
east and west walls (left), and east–west components for sensors on the north and south walls (right) except for the subbasement sensor which is on the west wall. See Figure 1 for location of sensors. Vertical numbering on the right indicates floor number with “A” for basement and “B” for subbasement.

## North-South components, East side of building

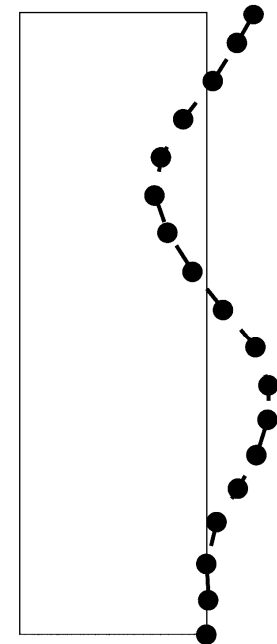
Mode 1



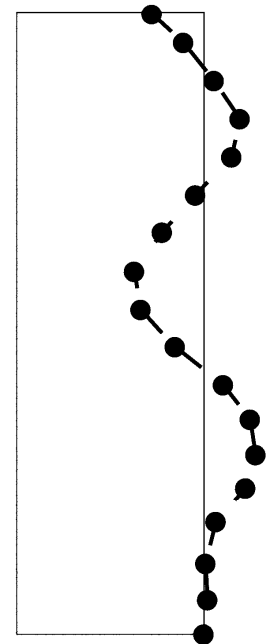
Mode 2



Mode 3

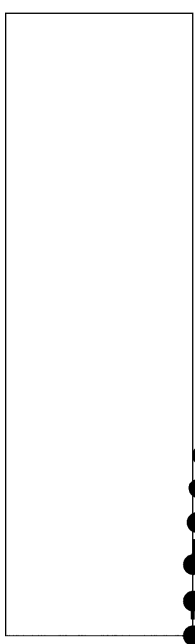


Mode 4

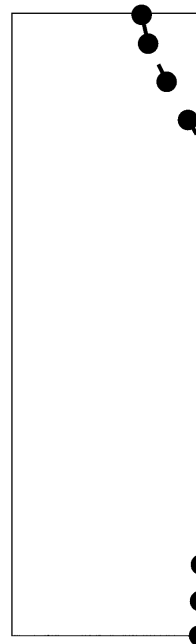


## East-West components, South side of building

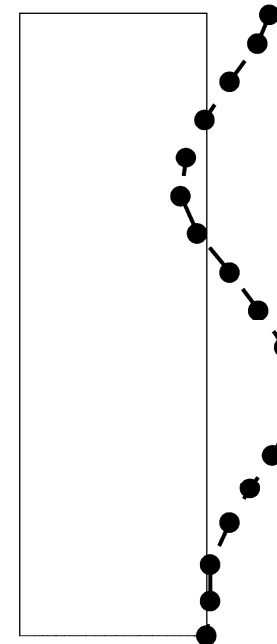
Mode 1



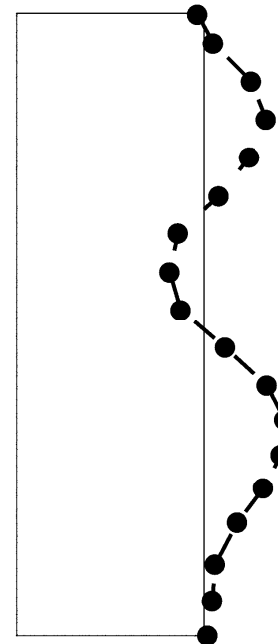
Mode 2



Mode 3

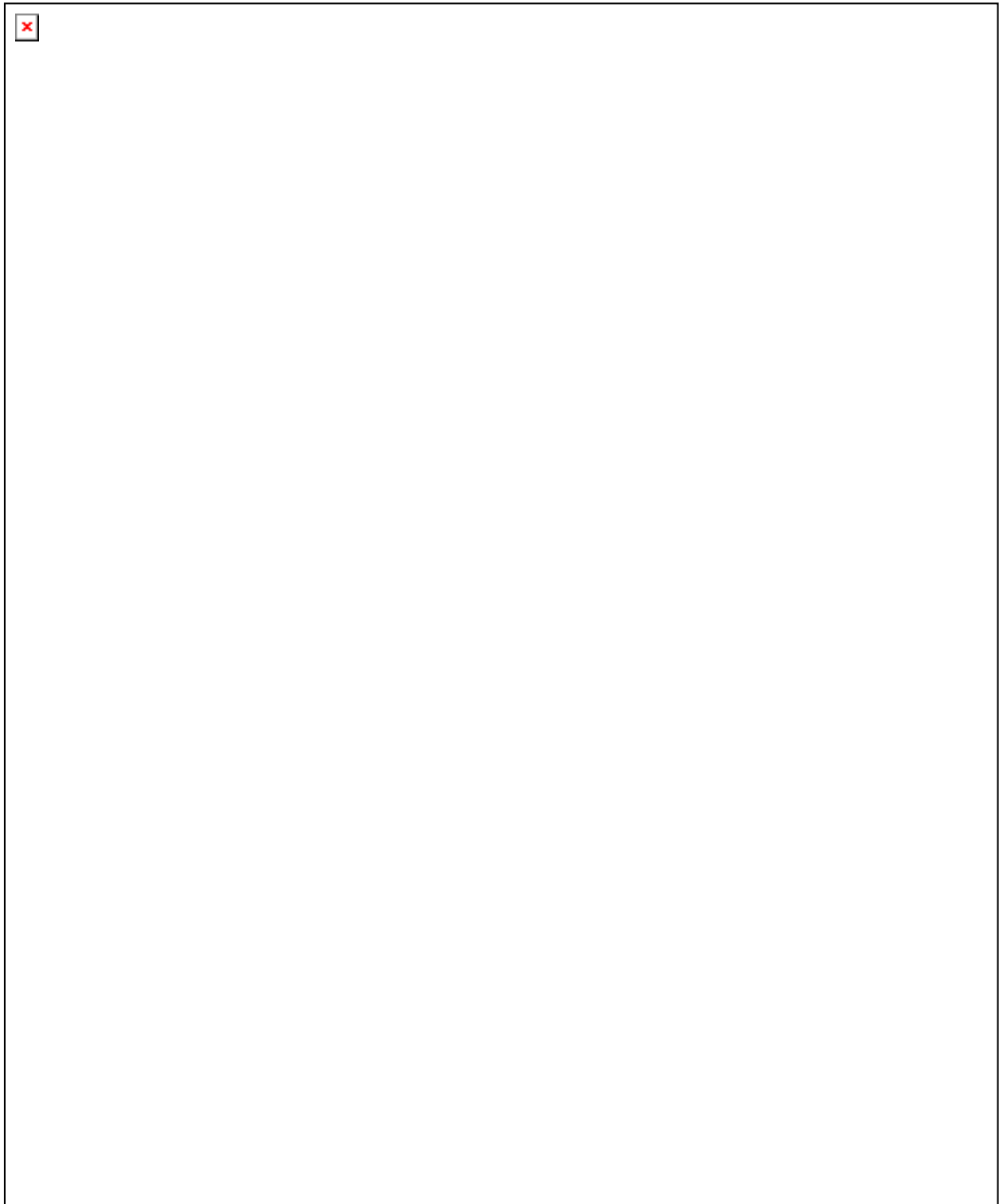


Mode 4



Mode shapes determined from narrowband  
filtered displacements recorded from the 16 December  
2004 Santa Monica Bay earthquake. Filled

circles represent actual sensor locations along the height of the building that contributed to the modeshape measurements.



Individual impulse response functions for four earthquakes. (a) 14 February 2004, (b) 21 February 2004 (3:39 UTC time), (c) 16 December 2004, and (d) 6 January 2005. See Table 1 for more information about these earthquakes. Each earthquake's pair

of plots shows the north-south components for sensors on the east wall (top) and east-west components for sensors on the south wall, except for the subbasement sensor which is on the west wall. For clarity, we show only those walls that had a subbasement sensor.

In chapter 4, we saw that the solution to this problem can be written as a sum of reflecting pulses. The motion in the building is given by

$$u_1(t, x_3) = u_1^g\left(t - \frac{x_3}{c}\right) + u_1^g\left(t - \frac{2h}{c} + \frac{x_3}{c}\right) - u_1^g\left(t - \frac{2h}{c} - \frac{x_3}{c}\right) \\ - u_1^g\left(t - \frac{4h}{c} + \frac{x_3}{c}\right) + u_1^g\left(t - \frac{4h}{c} - \frac{x_3}{c}\right) + \dots \quad (6.34)$$

where  $c$  is the shear-wave velocity in the building and  $u_1^g(t)$  is the horizontal motion of the ground at the base of the building. Notice that this sequence repeats with periodicity  $\frac{4h}{c}$ , which is the fundamental period of the building oscillation. We are particularly

interested in the drift in the building  $\varepsilon_{13}$ , which we can calculate from (6.34).

$$\varepsilon_{13}(t, x_3) = \frac{1}{c} \left[ -\dot{u}_1^g\left(t - \frac{x_3}{c}\right) + \dot{u}_1^g\left(t - \frac{2h}{c} + \frac{x_3}{c}\right) + \dot{u}_1^g\left(t - \frac{2h}{c} - \frac{x_3}{c}\right) \right. \\ \left. - \dot{u}_1^g\left(t - \frac{4h}{c} + \frac{x_3}{c}\right) - \dot{u}_1^g\left(t - \frac{4h}{c} - \frac{x_3}{c}\right) + \dots \right] \quad (6.35)$$

We are especially interested in the drift at the base of the building ( $x_3 = 0$ ), or

$$\varepsilon_{13}^b(t) = \frac{1}{c} \left[ -\dot{u}_1^g(t) + 2\dot{u}_1^g\left(t - \frac{2h}{c}\right) - 2\dot{u}_1^g\left(t - \frac{4h}{c}\right) + \dots \right] \quad (6.36)$$

That is at the base of the building, the up- and down-going waves interfere destructively to give zero displacement (remember it's a rigid base), but the associated strains interfere constructively to give twice as large a drift. Notice that the drift at the top of the building is zero, even though the motion is twice as large as in the rest of the building.

The actual drift in the base of our shear beam depends on the nature of the ground velocity  $\dot{u}_1(t)$ . Although strong shaking in earthquakes can take a wide variety of forms, it is common that ground displacements near large ruptures have motions described by a pulse of displacement (sometimes referred to as the “killer pulse”), or in other cases they may be dominated by the permanent offset of the ground with respect to an inertial reference frame. Consider the simple ground motions shown in Figure 6.22. The ground accelerations consist of a sequence of positive and negative constant steps. This results in ground velocity that consists of a number of linear ramps. The solution to this problem is simple as long as the duration of the pulse is shorter than the time required for the wave to travel up the building and then return  $\left(\frac{2h}{c}\right)$ . Things get more complex when the

duration of the ground motion becomes large. Of interest is the maximum shear strain at the base of the building, which we can write as

$$\left| \varepsilon_{13}^b \right|_{\max} = \frac{\left| \dot{u}_g \right|_{\max}}{c} A \quad (6.37)$$

where  $A$  is an amplification factor. For ground motions A and B,  $A$  depends on  $T_p/T_1$ , where  $T_1 = 4h/c$  is the fundamental period of the building. The factor  $A$  reaches 2 for ground motion A (when  $T_p \leq T_1$ ) and 4 for ground motion B (when  $T_p = T_1$ ). Plots of  $\varepsilon_{13}^b(t)$  for  $T_p = T_1$  are shown in Figure 6.23. The configurations of the building at different times are shown in Figure 6.24.

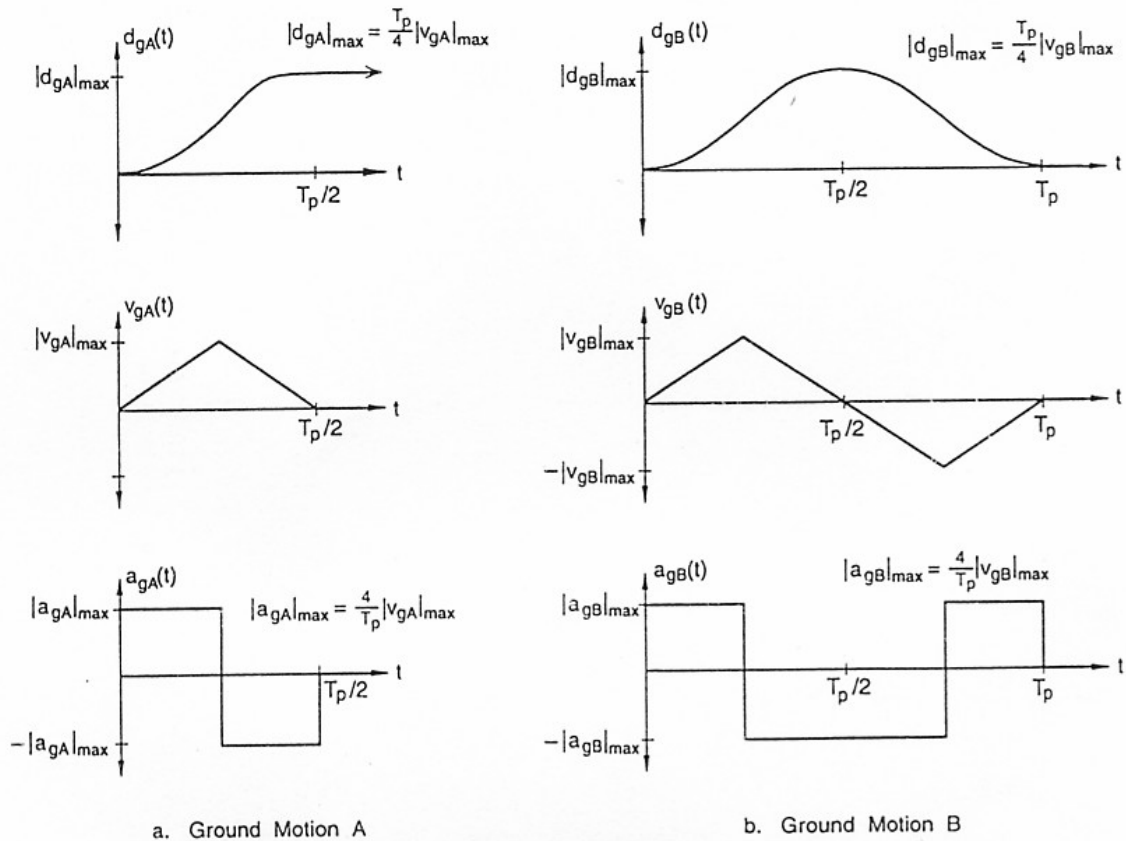


Figure 6.22. Simple ground motions that consist of a simple static displacement (case A) and a pulse of displacement (case B).

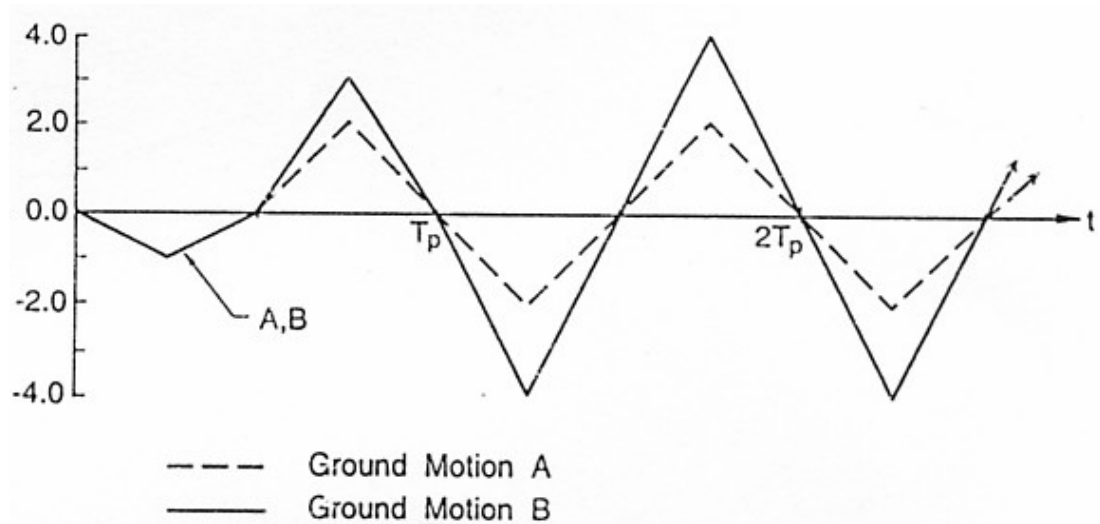


Figure 6.23. Shear strain in the base of the building. One unit on the vertical axis corresponds to a strain of  $\frac{c\varepsilon_{13}^b(t)}{\dot{u}_g|_{\max}}$ .

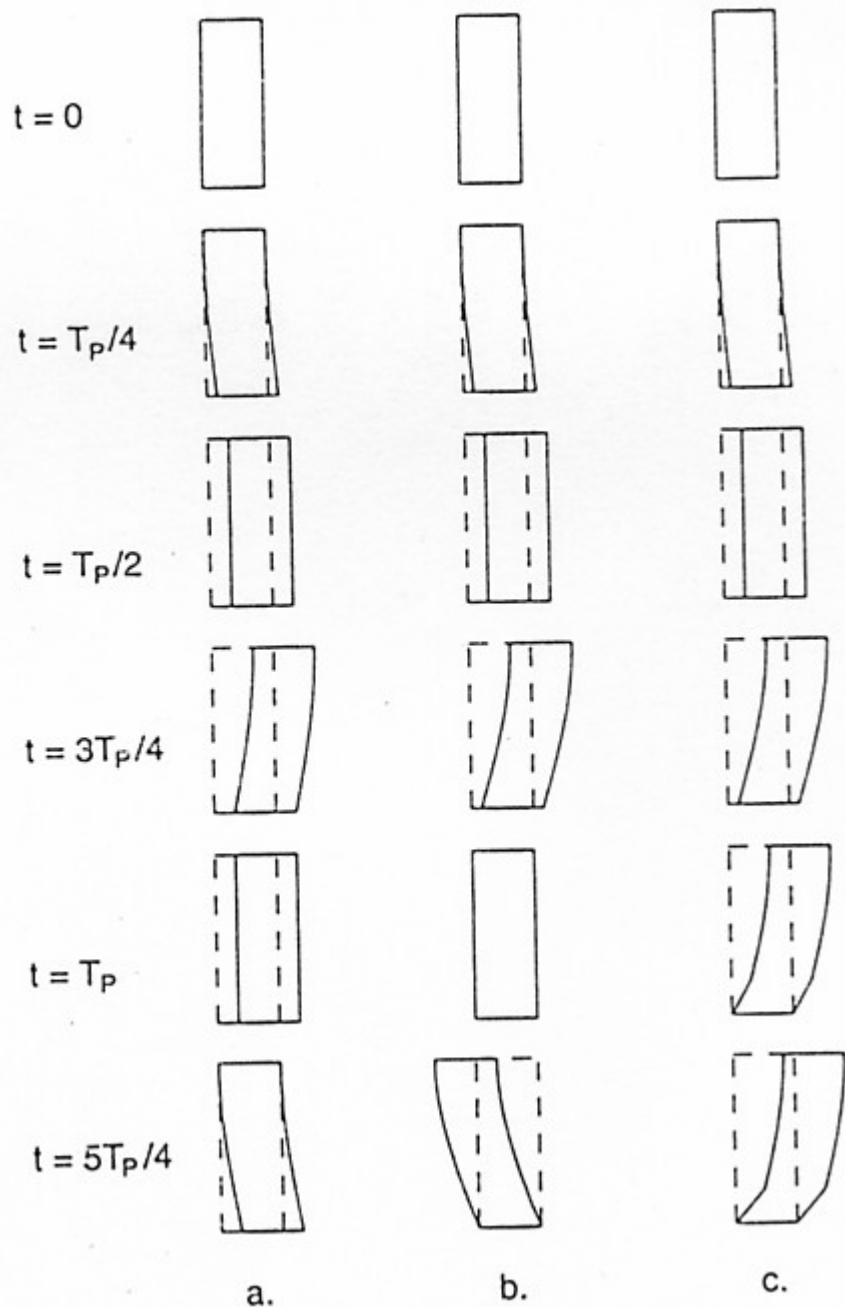


Figure 6.24. Configuration of a multi-story building at time intervals of  $T_p/4$  for the case  $T_p = T_1$ . a) Elastic shear beam building for ground motion A. b) Elastic shear beam building for ground motion B. c) Inelastic shear beam building for ground motion B (qualitative depiction).

The shear strain  $\left| \varepsilon_{13}^b \right|_{\max}$  can be large enough to be well into the inelastic range. With  $\left| \dot{u}_g \right|_{\max} = 1 \text{ m/s}$ , and  $c = 100 \text{ m/s}$  (a typical value for a tall building), we can use (6.37) and

Figure 6.23 to calculate that  $|\varepsilon_{13}^b|_{\max} = 0.02$  for ground motion A and 0.04 for ground motion B, when  $T_p = T_1$ . These are large values and can greatly exceed the yield strain at the base of the building (e.g., check out Figure 6.6).

The dynamics problem becomes far more complex when the building experiences yielding. That is the governing equations are no longer linear and it is generally necessary to perform a careful finite-element analysis to understand the deformation of the structure. Such an analysis was performed by Hall and others (1995), and the typical results are shown in Figure 6.25. Figure 6.26 shows the location of weld failures (moment resisting connections) in the structure.

When the building yields, it tends to develop a permanent bend in the structure. Once a tall frame building is permanently bent, there is really no practical way to straighten it again, and it is a total loss. Furthermore, if the bending exceeds several percent locally, then there may be a real fear of collapse due to P-Δ effects.

Figure 19

Perspective view of the 20-story building responding to the C5 ground motion at the times A, B, C, D and E marked in Figure 17. A: Building is at rest before ground displacement pulse arrives. B: Forward phase of the pulse. Building is moving forward, but lagging in the upper stories. C: Ground has reached its maximum displacement. Most of the building is moving rapidly forward. D: Back phase of the pulse. Upper portion of the building is still moving forward. E: End of the ground-displacement pulse. Offsets remain in the lower half of the building.

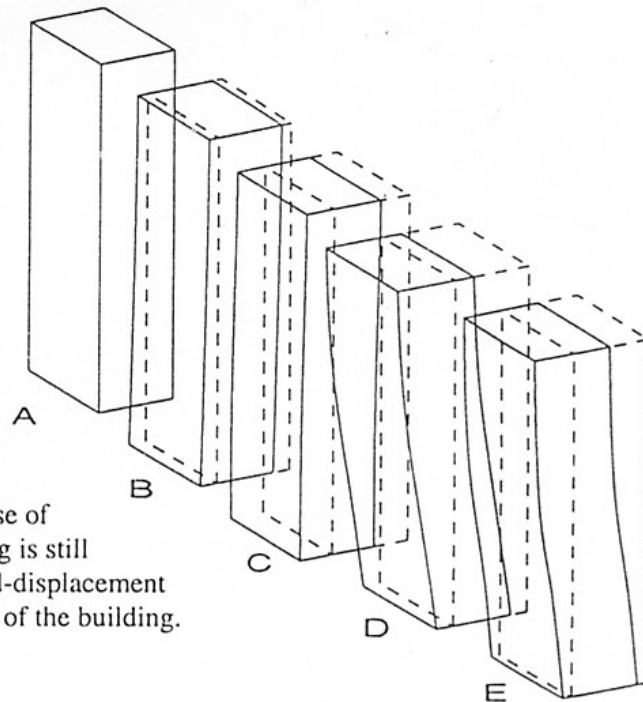


Figure 6.25 From Hall and others (1995).

One way to gain some insight into the behavior of a yielding beam is to consider the building as if it were linear, but with a local stiffness that changes with the amplitude of the local drift. For example, the slope of the force-drift curve in Figure 6.6 is called the tangent stiffness, and it rapidly decreases when the building begins to yield (it even changes sign). Since the stiffness is critical in determining the velocity at which a deformation propagates up a building, loss of stiffness due to yielding means that deformations tend to slow their propagation up a building. That is, once yielding begins,

deformations tend to localize in these yielding zones. Perhaps an example of this is shown in Figure 6.27 in which an 8-story building lost the 6<sup>th</sup> story during the 1995 Kobe earthquake. That is, when ground motions are propagating in a building, then once yielding begins at a particular place, then that is where the majority of the strain will occur.

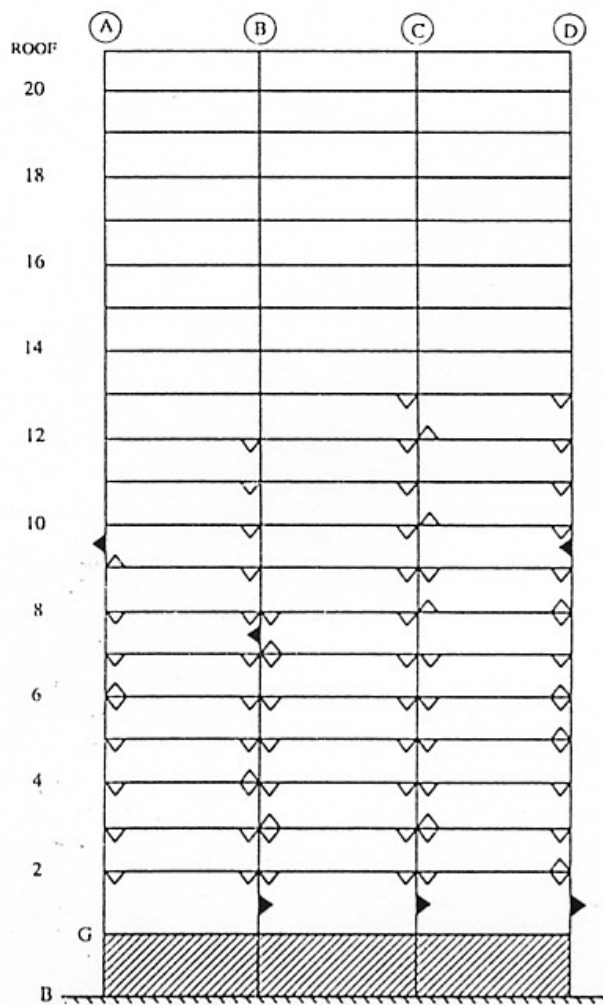


Figure 6.26 Distribution of weld fractures in a 20 story building caused by a 2 meter displacement pulse as reported by Hall and others (1995). A dark triangle locates a cracked column-flange weld at a column splice due to tension in the column. These can be very serious, since if the column separates in tension, but does not come back together properly, the column may fail to carry the weight of the building (very bad). Open triangles locate failed moment-frame connections, which causes a loss of ductility, but is not as serious as failure of a column splice.

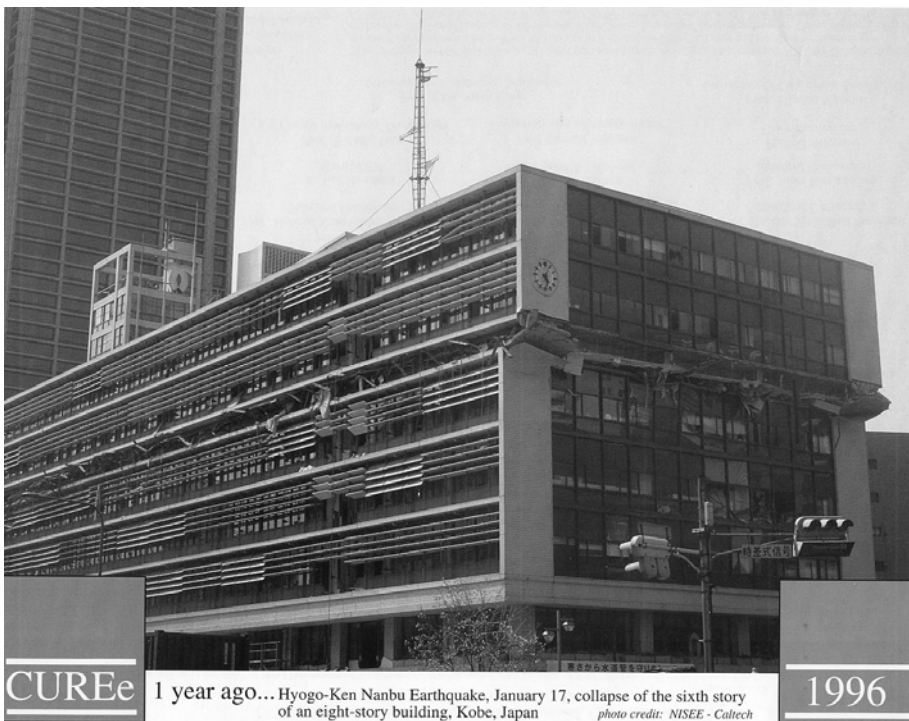
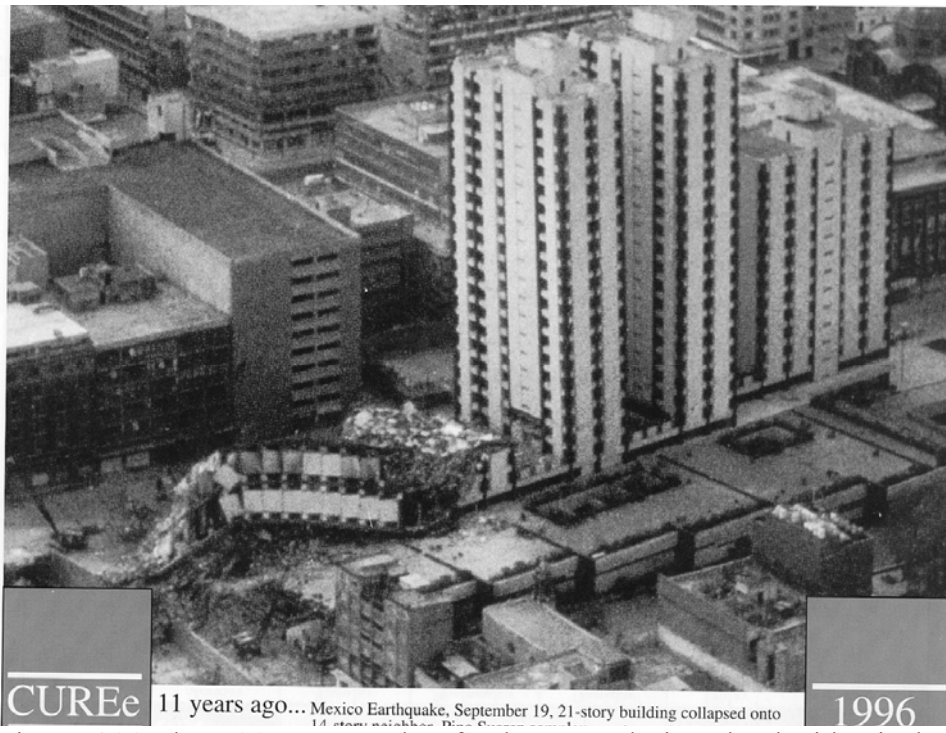


Figure 6.27. Once yielding begins at some location, then the loss of stiffness at that location can tend to localize the deformations to that location. This may have been the cause of the collapse of the 6<sup>th</sup> floor of this 8-story building in Kobe in 1995.

Prediction of the collapse of structures is extremely difficult. That is, the failure of a critical component (such as a weld) may cause loads carried by a structural element to be transferred to others structural elements, which may cause a cascade of failures.

Assessing the likelihood of failure means obtaining an accurate understanding of all of these interrelations (highly nonlinear and perhaps chaotic). Consider the three identical 21-story steel mrf towers in Mexico City that experienced the 1995 Michoacan earthquake (Figure 6.28 and 6.29). This was not a failure due to the propagation of a displacement pulse. Instead, it was due to amplification of 2-second ground motions by the shallow sediments beneath Mexico City (see Chapter 4).

Although the three towers were designed to be the same, their behavior was quite different, despite their close proximity to each other. The tower on the right suffered no apparent damage as a result of the shaking. The tower on the left collapsed, while the tower in the middle had a permanent roof drift of about 1 meter. It would be very difficult to explain this difference by current state of the art in numerical modeling of these buildings.



CUREe

11 years ago...Mexico Earthquake, September 19, 21-story building collapsed onto

1996

Figure 6.28 Three 21-story steel mrf's that were designed to be identical. The left tower collapsed, the middle tower had a 1-meter permanent drift of its roof, and the right tower suffered no apparent damage. (Mexico City following the 1985 Michoacan earthquake).



CUREe

14 years ago...Mexico (Michoacan) Earthquake, September 19, 1985: Collapse of a 21-story building with steel box-column frames and X-braces. The 21-story building collapsed onto an adjacent 14-story building at the Pino Suarez Complex in Mexico City.

1999

Figure 6.29. Close-up of the left tower in Figure 6.28.

### Soil-Structure Interaction for a Shear Beam

As long as we are treating the shear-beam building as if it was a low-velocity, low-density layer on the top of the Earth, we can gain some insight into how the building interacts with the soil layers. For instance, we can ask 1) how much does the presence of the building change the ground motion at its base compared to the ground motion that would have occurred without the presence of the building (a free field site), and 2) how much of the motion of the building is transmitted through the base of the building when a wave reflects off the top of the building and then transmits through the base of the building?

From Chapter 4 we know that for an SH-wave vertically incident on a the base of a layer of buildings,

$$\begin{aligned} \frac{A_B^T}{A_G^I} &= \frac{2\mu_G\beta_B}{\mu_G\beta_B + \mu_B\beta_G} \\ &= \frac{2\beta_B\rho_B}{\beta_G\rho_G + \beta_B\rho_B} \approx 2 \left[ 1 - \frac{\beta_B\rho_B}{\beta_G\rho_G} + \left( \frac{\beta_B\rho_B}{\beta_G\rho_G} \right)^2 + \dots \right] \end{aligned} \quad (6.38)$$

where  $A_B^T$  is the amplitude of the wave transmitted into the building and  $A_G^I$  is the amplitude of the incident wave from the ground. Let us suppose that the shear wave velocity in the soil is approximately twice that in the building (a fairly soft soil), and that the density of the building is 5% of the density of the soil, then

$$\frac{A_B^T}{A_G^I} \approx 2(1 - 0.025) = 1.975 \quad (6.39)$$

But the amplitude of the motion without the building is 2.0 because it is an SH reflection off of the free surface. Therefore the building causes the amplitude of the motion to be decreased by 1 ¼ % relative to the ground motion that would have occurred without the presence of the building. This soil-structure interaction effect seems to be far less important than the effect of allowing the building to rock on its foundation.

We can also compute the size of the wave reflected off the base of the building  $A_B^R$  compared with the amplitude of the downgoing wave in the building  $A_B^I$ . That is

$$\begin{aligned} \frac{A_B^R}{A_B^I} &= \frac{\beta_B\mu_G - \beta_G\mu_B}{\beta_B\mu_G + \beta_G\mu_B} \\ &= \frac{\mu_G^2\mu_B\rho_G - \mu_B^2\mu_G\rho_B}{\mu_G^2\mu_B\rho_G + \mu_B^2\mu_G\rho_B + 2\mu_G\mu_B\sqrt{\mu_G\mu_B\rho_G\rho_B}} \end{aligned} \quad (6.40)$$

If the density of the ground is large compared to the building ( $\rho_G \gg \rho_B$ ), then

$$\begin{aligned}
\frac{A_B^R}{A_B^I} &\approx \frac{\mu_G^2 \mu_B \rho_G - \mu_B^2 \mu_G \rho_B}{\mu_G^2 \mu_B \rho_G} \\
&= 1 - \frac{\rho_B \mu_B}{\rho_G \mu_G} \\
&= 1 - \left( \frac{\rho_B \beta_B}{\rho_G \beta_G} \right)^2
\end{aligned} \tag{6.41}$$

Therefore, most of the wave is reflected off the base of the building. For the previous case, the reflected wave is 99.94% the amplitude of the incident wave.

## Bending Beam

It is not possible to solve the bending beam problem in the same way that we did the shearing beam. For technical theory of bending, the horizontal displacements of the building obey the Bernoulli-Euler equation, which is

$$EI \frac{\partial^4 u_1(x_3, t)}{\partial x_3^4} = -\rho S \frac{\partial^2 u_1(x_3, t)}{\partial t^2} \tag{6.42}$$

where  $S$  is the cross-sectional area of the building ( $= w^2$  if the building has a square cross section). Whereas Navier's equation was a second order equation, the Bernoulli-Euler bending beam equation is a fourth order equation. Fortunately, this is still a linear equation. However, it is no longer true that there is a unique velocity such that  $u_1 = f(t - x_3/c)$  solves this equation. We can try a traveling harmonic wave; that is assume that

$$u_1 = \sin(k_n x - \omega_n t) \tag{6.43}$$

Direct substitution indicates that (6.43) is a solution to (6.42) if

$$\frac{\omega_n}{k} = \sqrt{\omega_n} \sqrt[4]{\frac{EI}{\rho S}} \tag{6.44}$$

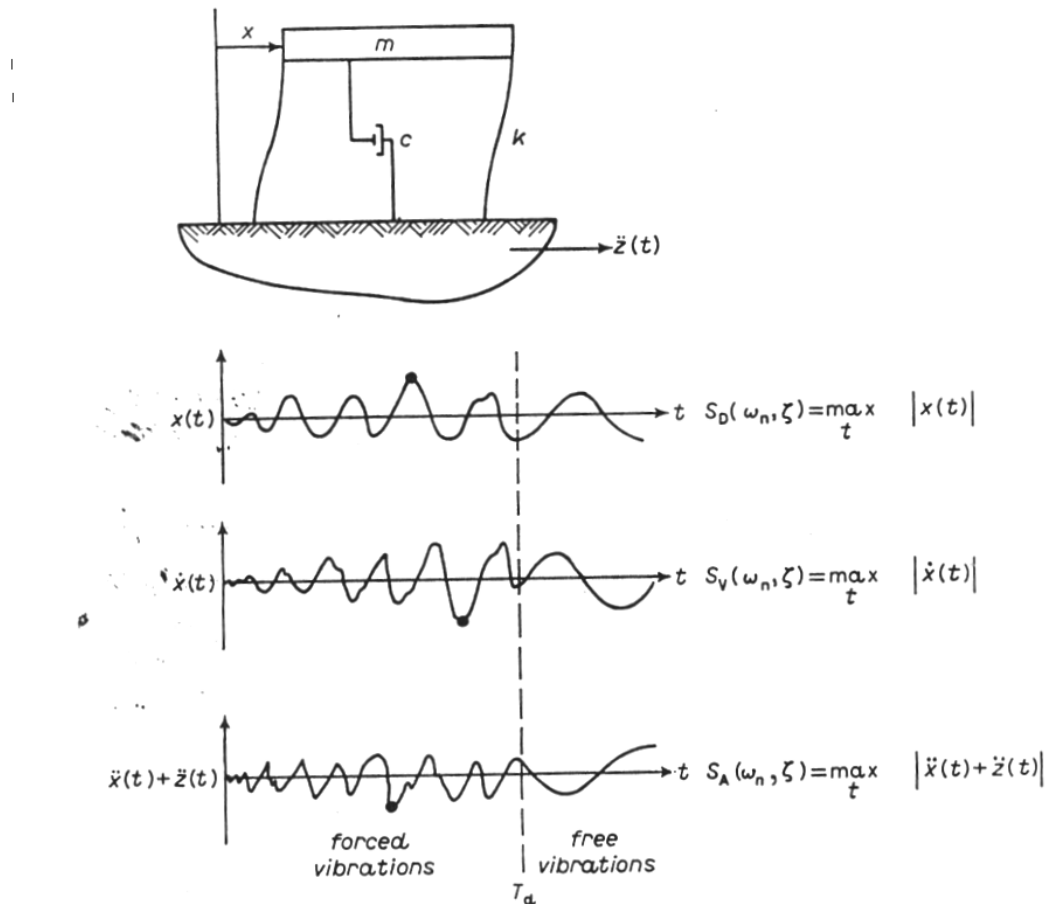
But  $\omega_n/k_n$  is just the phase velocity  $c_n$  of this traveling harmonic wave. Therefore, we see that the phase velocity of a traveling harmonic waves increases as the square root of the frequency of the wave. Since (6.42) is linear, we can form a more general solution of the form

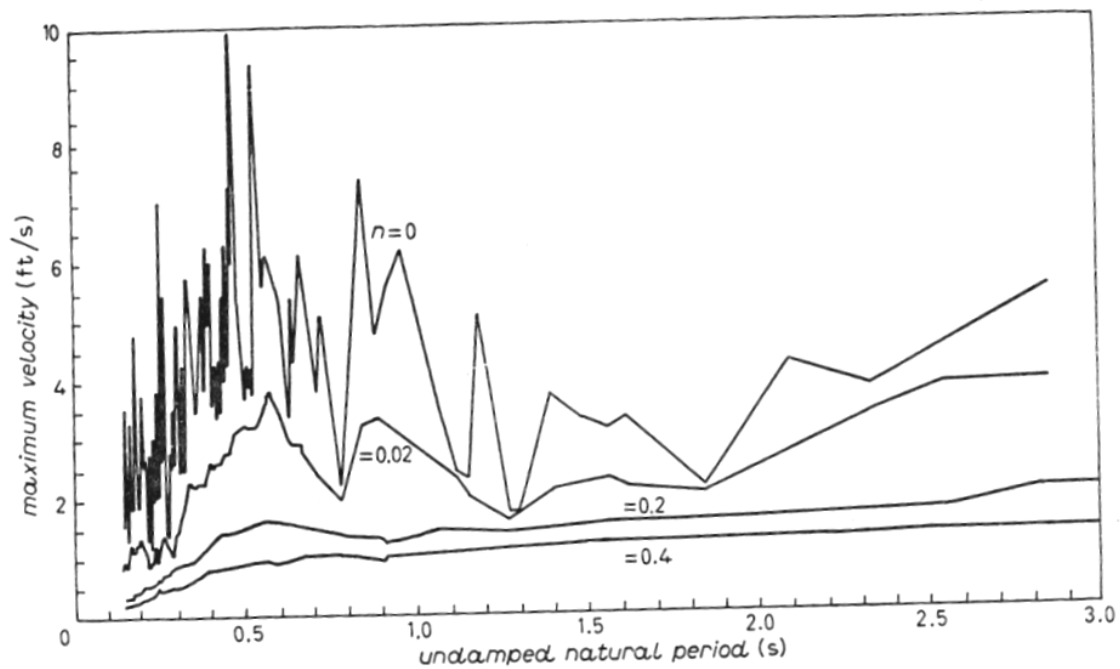
$$u_1 = \sum_n C_n \sin k_n (x - c_n t) \tag{6.45}$$

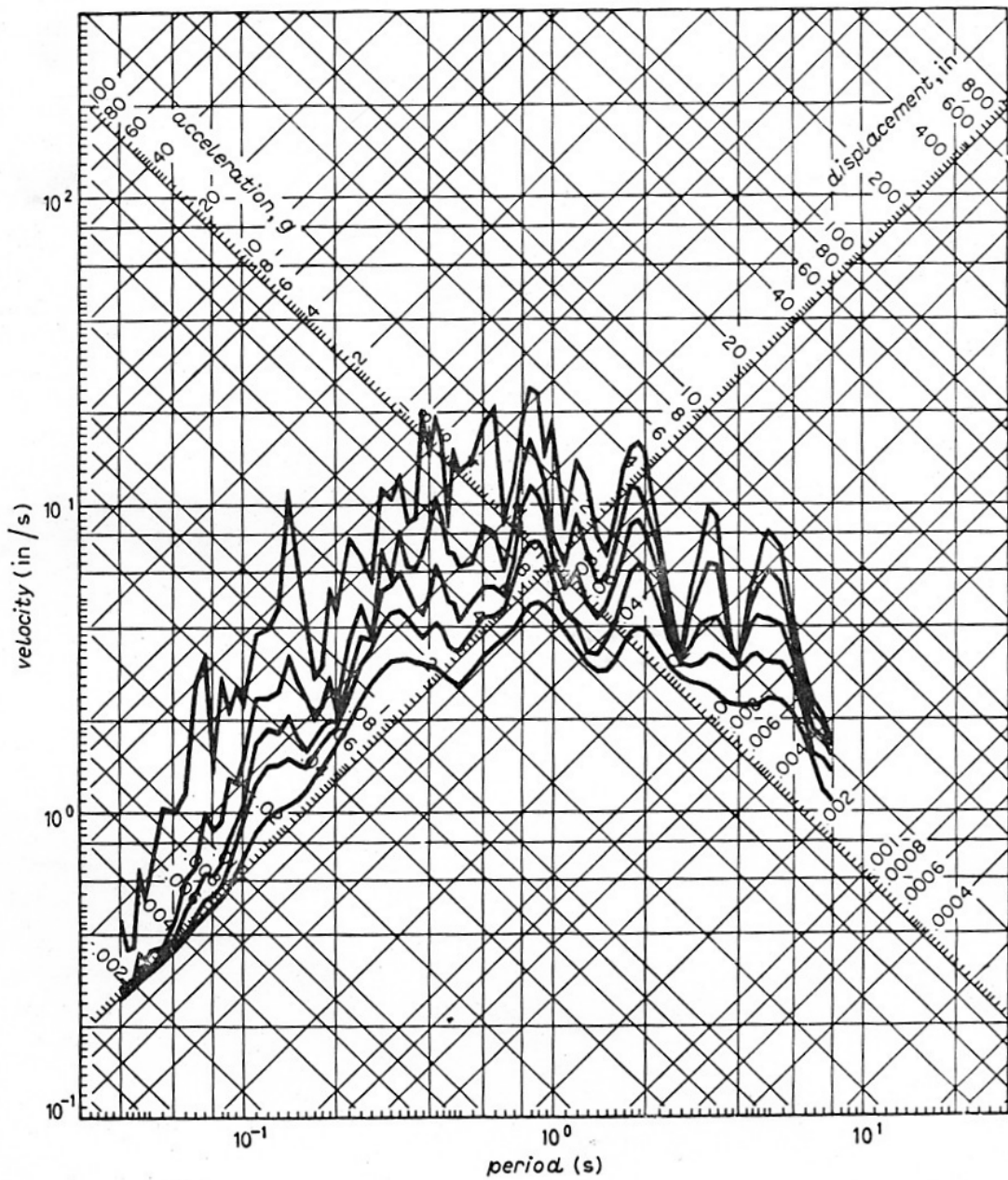
where the  $C_n$ 's are constants. Since the different frequencies travel at different velocities, the waveform will change as the wave propagates. This is known as dispersion. There is probably some dispersion that occurred in the propagation of the pulse in the building shown in Figure 6.21. This may explain why it becomes difficult to distinguish the pulse after it has propagated a long distance in the building.

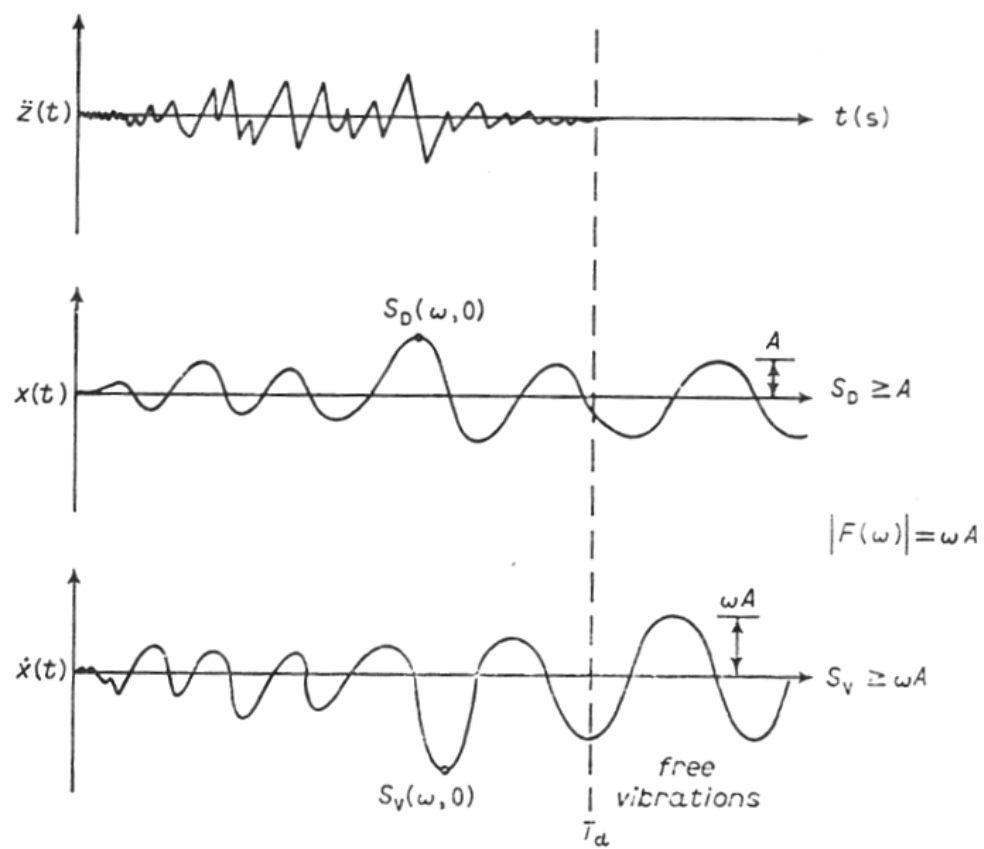
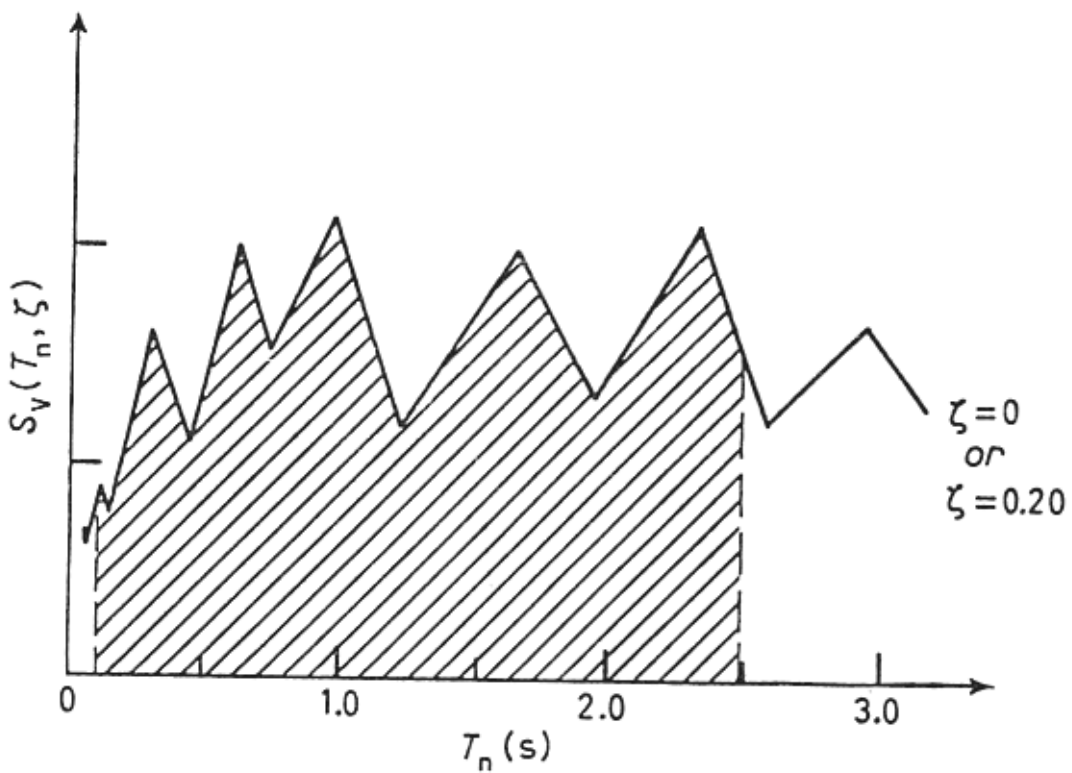
## Spectral Methods

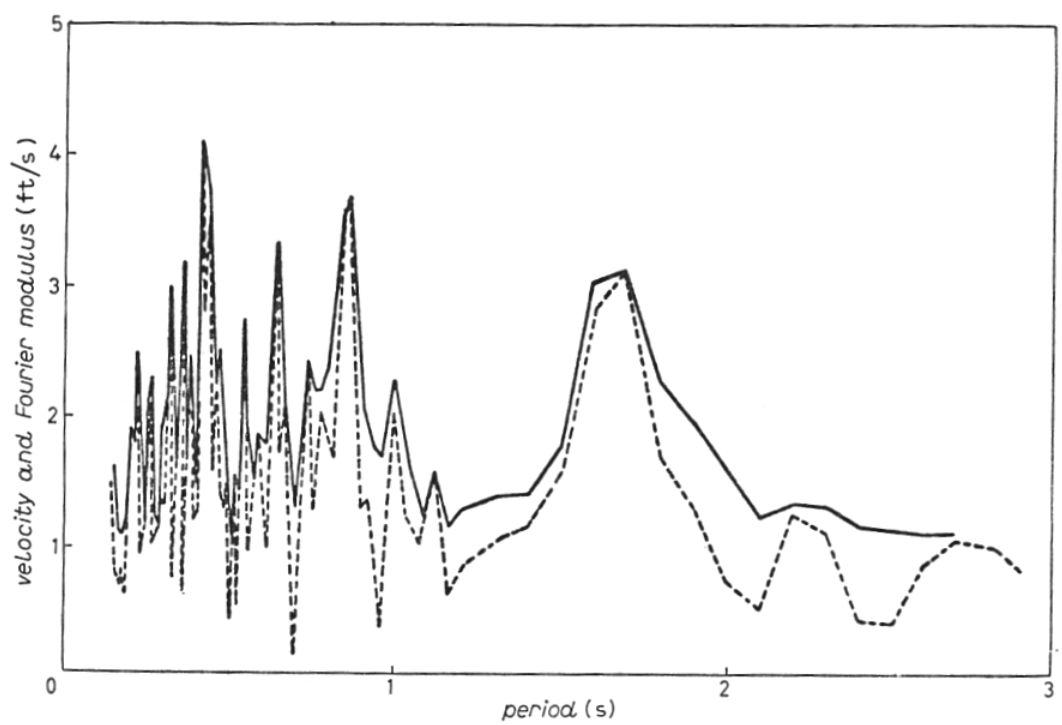
The problem of oscillations of a complex system of coupled linear oscillators can be quite complex to solve. However, it can be shown that for a linear system with  $n$  degrees of freedom that is oscillating about its static equilibrium, then the motion can be represented as the sum of  $n$  modes. In general, each mode has a particular frequency and mode shape associated with it. By summing the modes with the proper phase and amplitude, any possible motion of the system can be produced. Buildings are continuous systems, and therefore it would require an infinite set of modes to represent all the motions. However, a reasonable approximation can be achieved by representing the building with a number of discrete elements (e.g., the different floor slabs) that are coupled by spring elements (e.g., moment resisting connections).





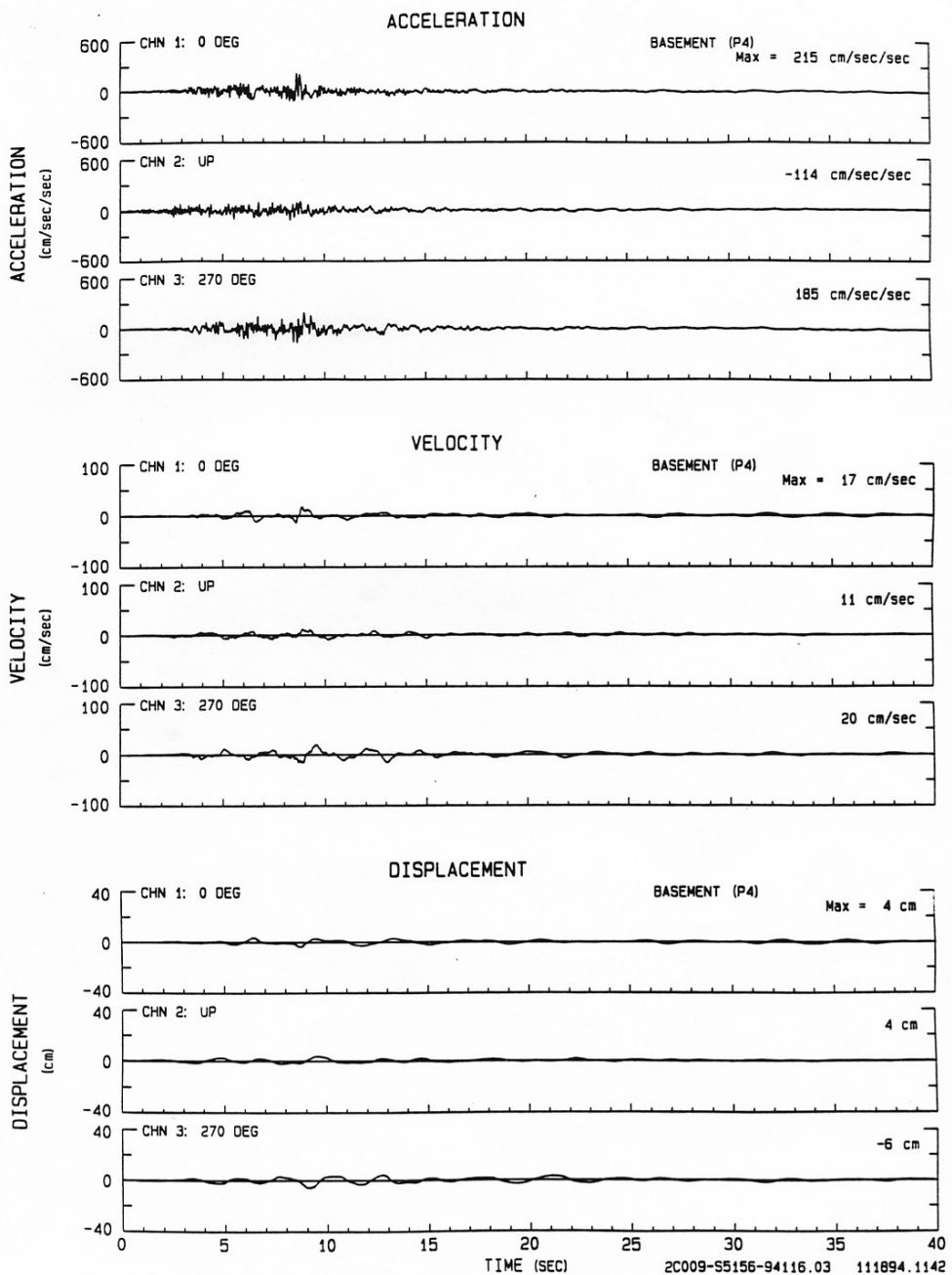




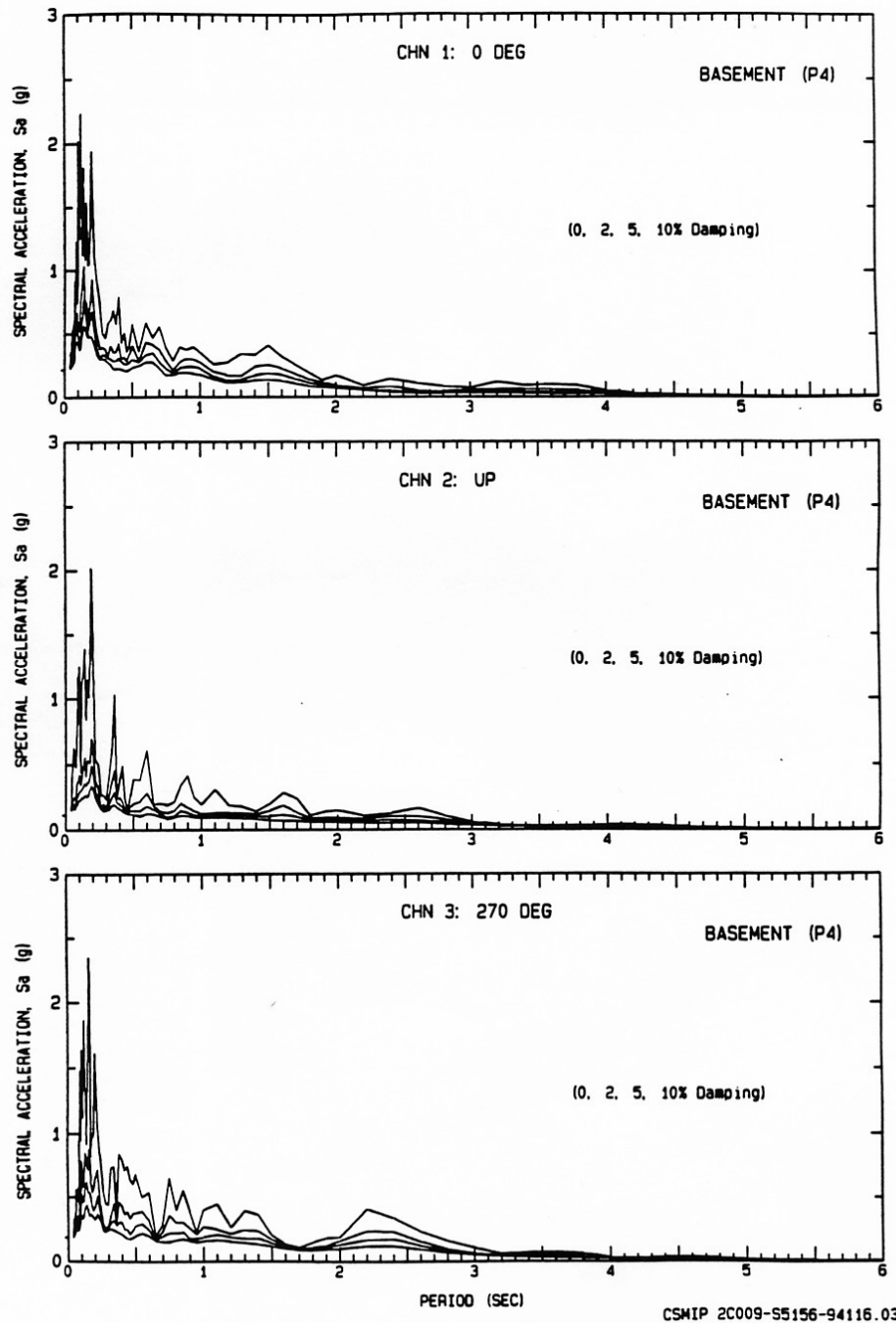


NORTHRIDGE EARTHQUAKE OF JAN 17, 1994 CSMIP PRELIMINARY PROCESSING  
LOS ANGELES - WILSHIRE BLVD #9 CSMIP Sta Num 2C009  
Usable Data Bandwidth: .17 to 23.6 Hz (.04 to 6.0 Sec)

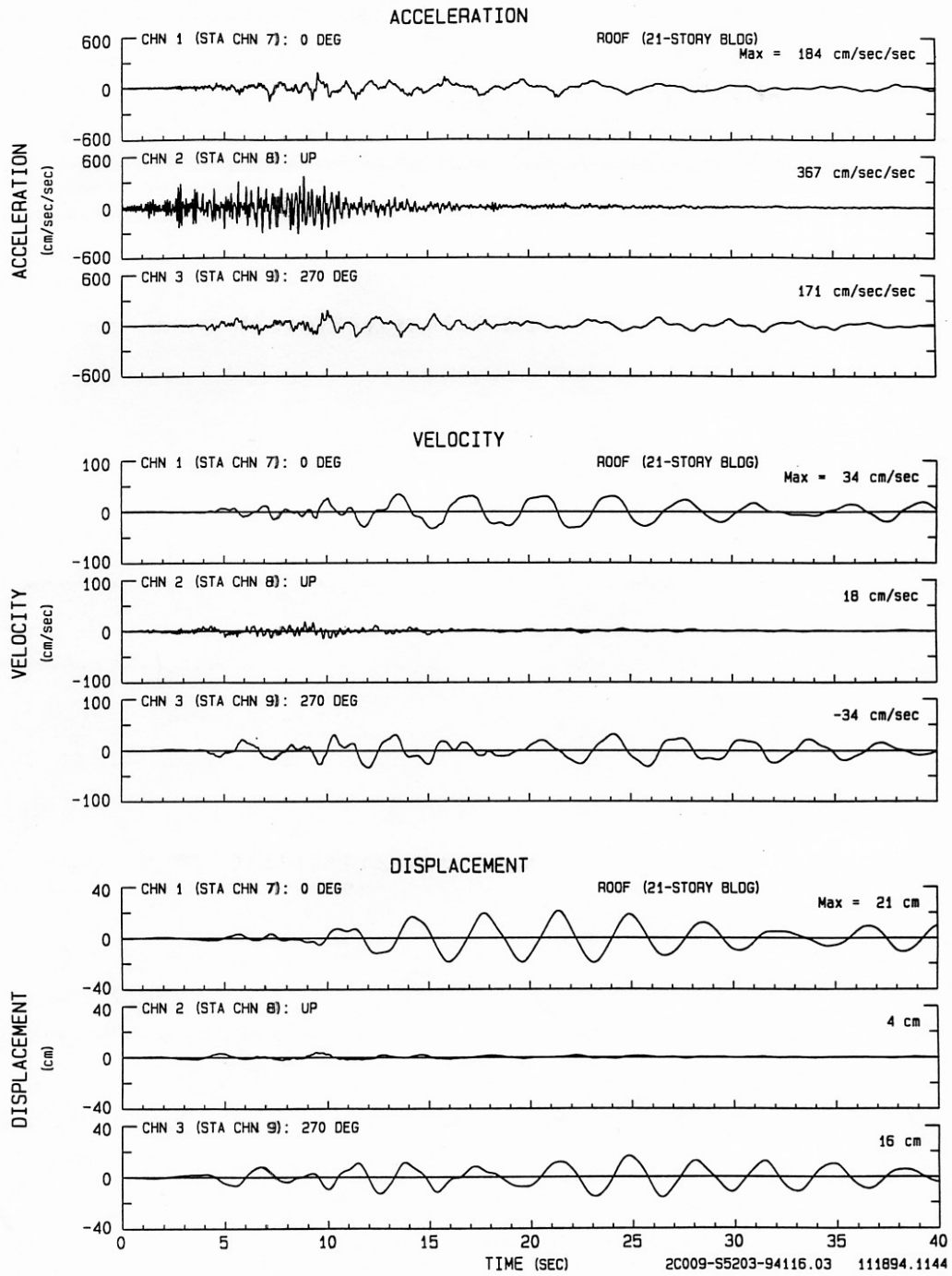
71



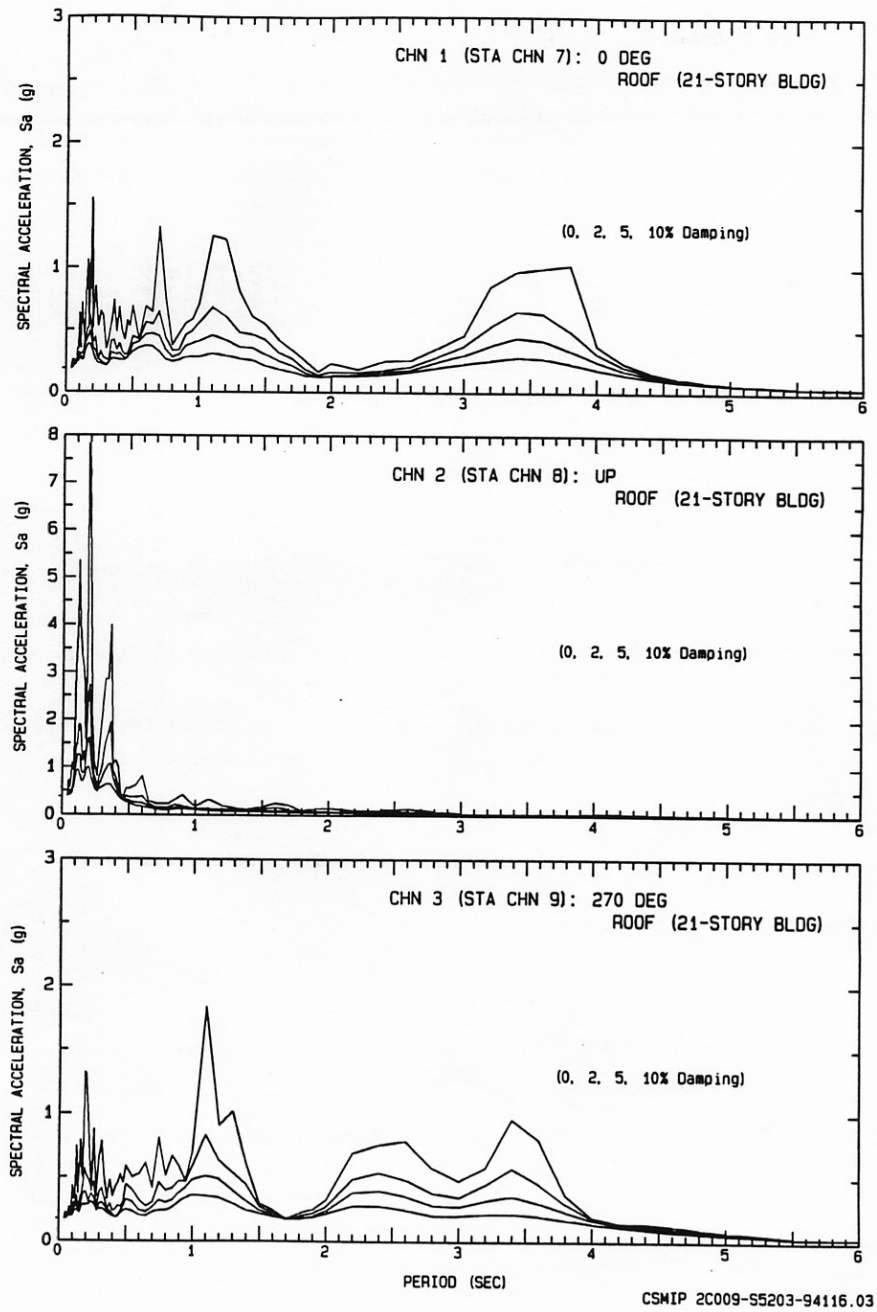
NORTHRIDGE EARTHQUAKE OF JAN 17, 1994      CSMIP PRELIMINARY PROCESSING  
LOS ANGELES - WILSHIRE BLVD #9   Sta Num 2C009  
USABLE DATA BANDWIDTH: .17 TO 23.6 Hz (.04 TO 6.0 SEC)



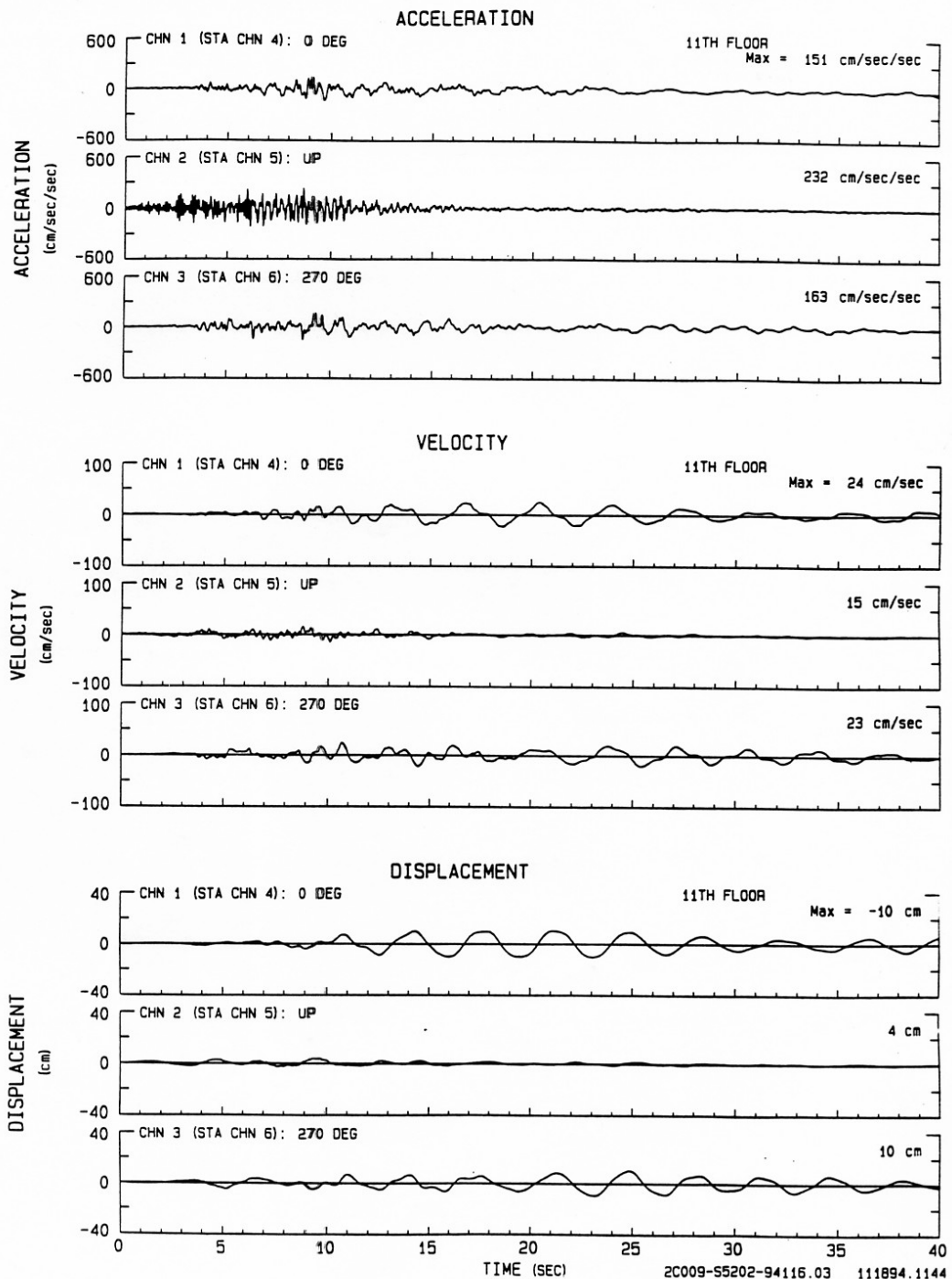
NORTHRIDGE EARTHQUAKE OF JAN 17, 1994      CSMIP PRELIMINARY PROCESSING  
 LOS ANGELES - WILSHIRE BLVD #9      CSMIP Sta Num 2C009  
 Usable Data Bandwidth: .17 to 23.6 Hz (.04 to 6.0 Sec)



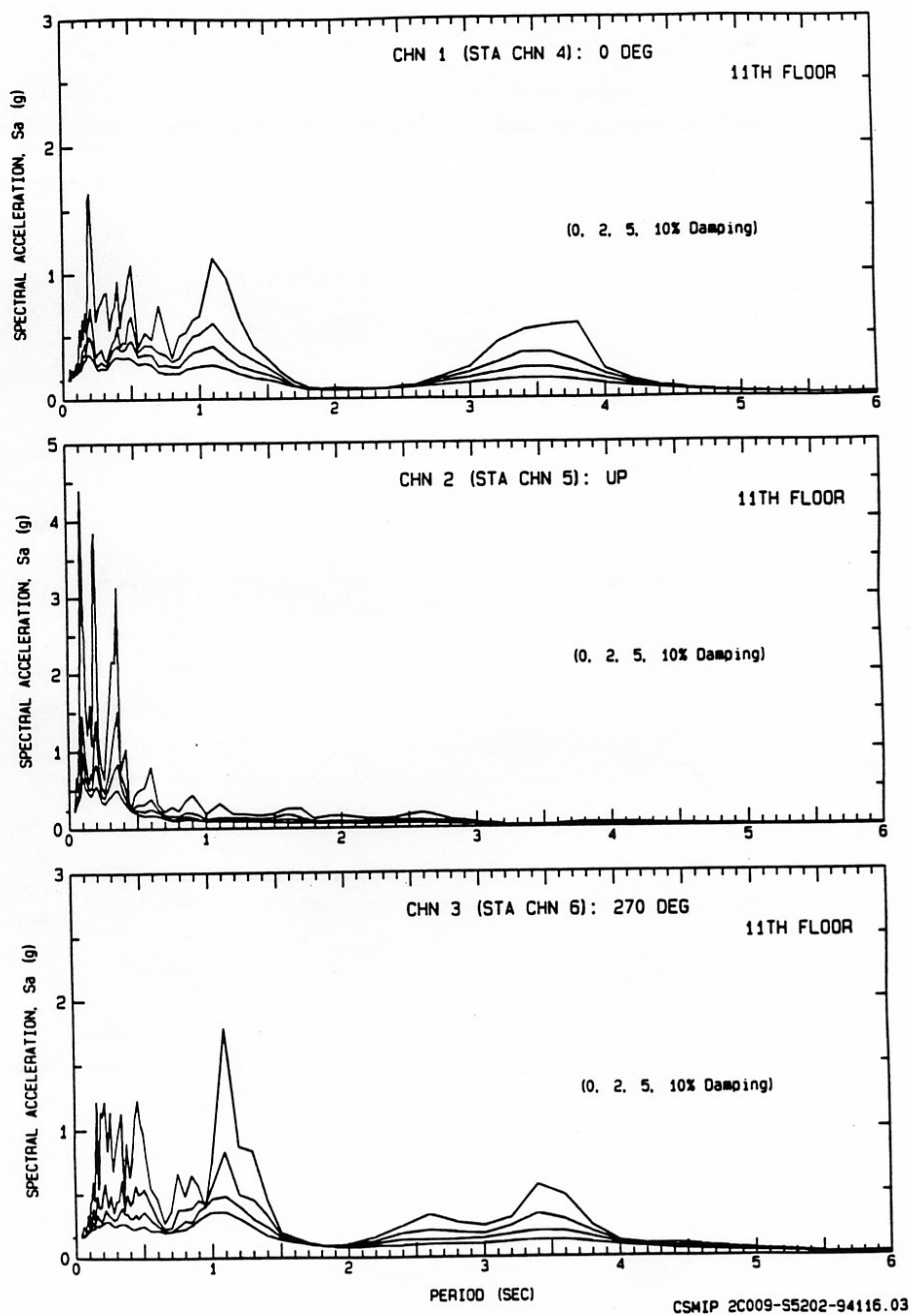
NORTHRIDGE EARTHQUAKE OF JAN 17, 1994      CSMIP PRELIMINARY PROCESSING  
LOS ANGELES - WILSHIRE BLVD #9 Sta Num 2C009  
USABLE DATA BANDWIDTH: .17 TO 23.6 Hz (.04 TO 6.0 SEC)



NORTHRIIDGE EARTHQUAKE OF JAN 17, 1994      CSMIP PRELIMINARY PROCESSING  
 LOS ANGELES - WILSHIRE BLVD #9      CSMIP Sta Num 2C009  
 Usable Data Bandwidth: .17 to 23.6 Hz (.04 to 6.0 Sec)



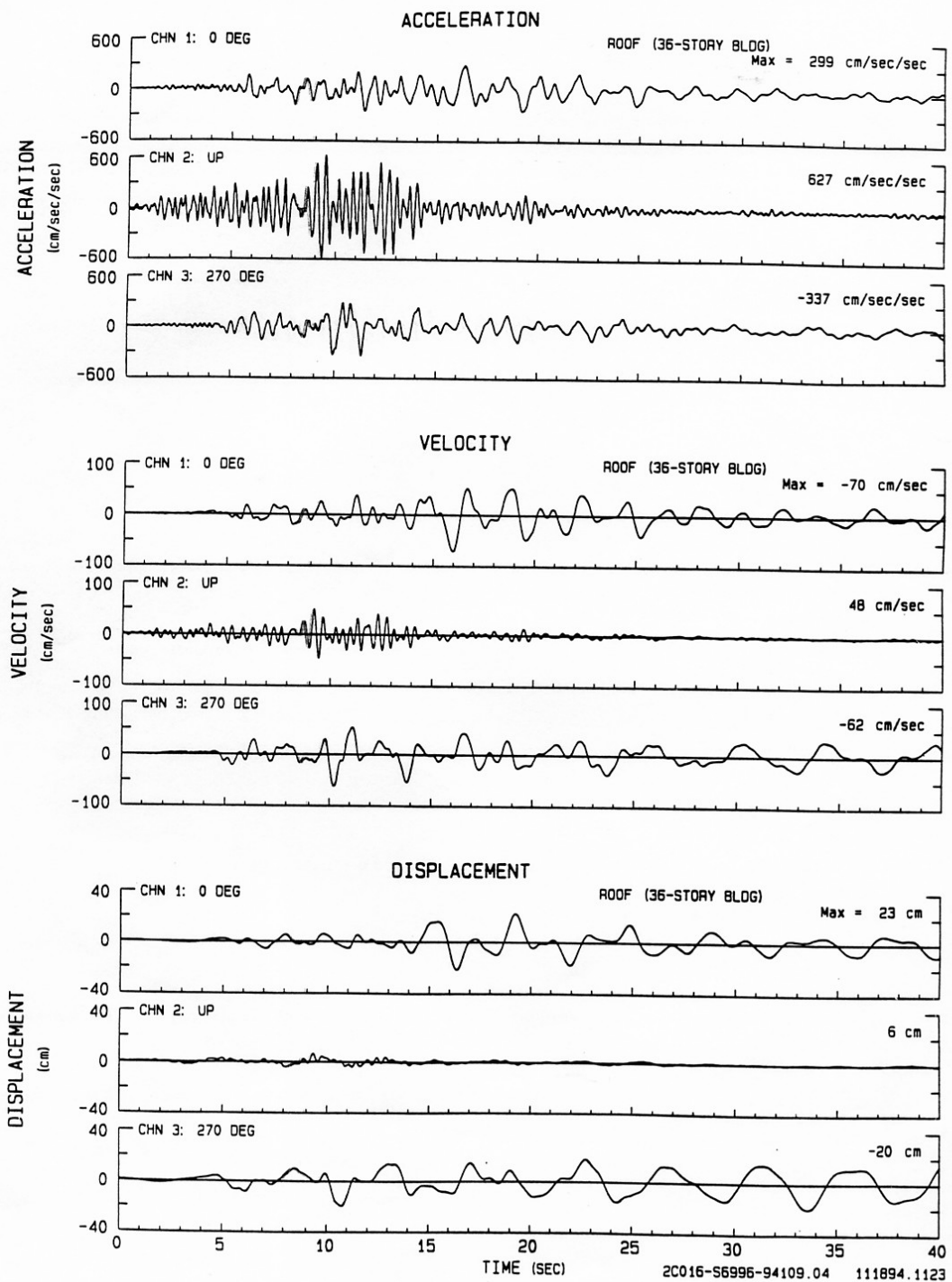
NORTHRIDGE EARTHQUAKE OF JAN 17, 1994      CSMIP PRELIMINARY PROCESSING  
LOS ANGELES - WILSHIRE BLVD #9 Sta Num 2C009  
USABLE DATA BANDWIDTH: .17 TO 23.6 Hz (.04 TO 6.0 SEC)



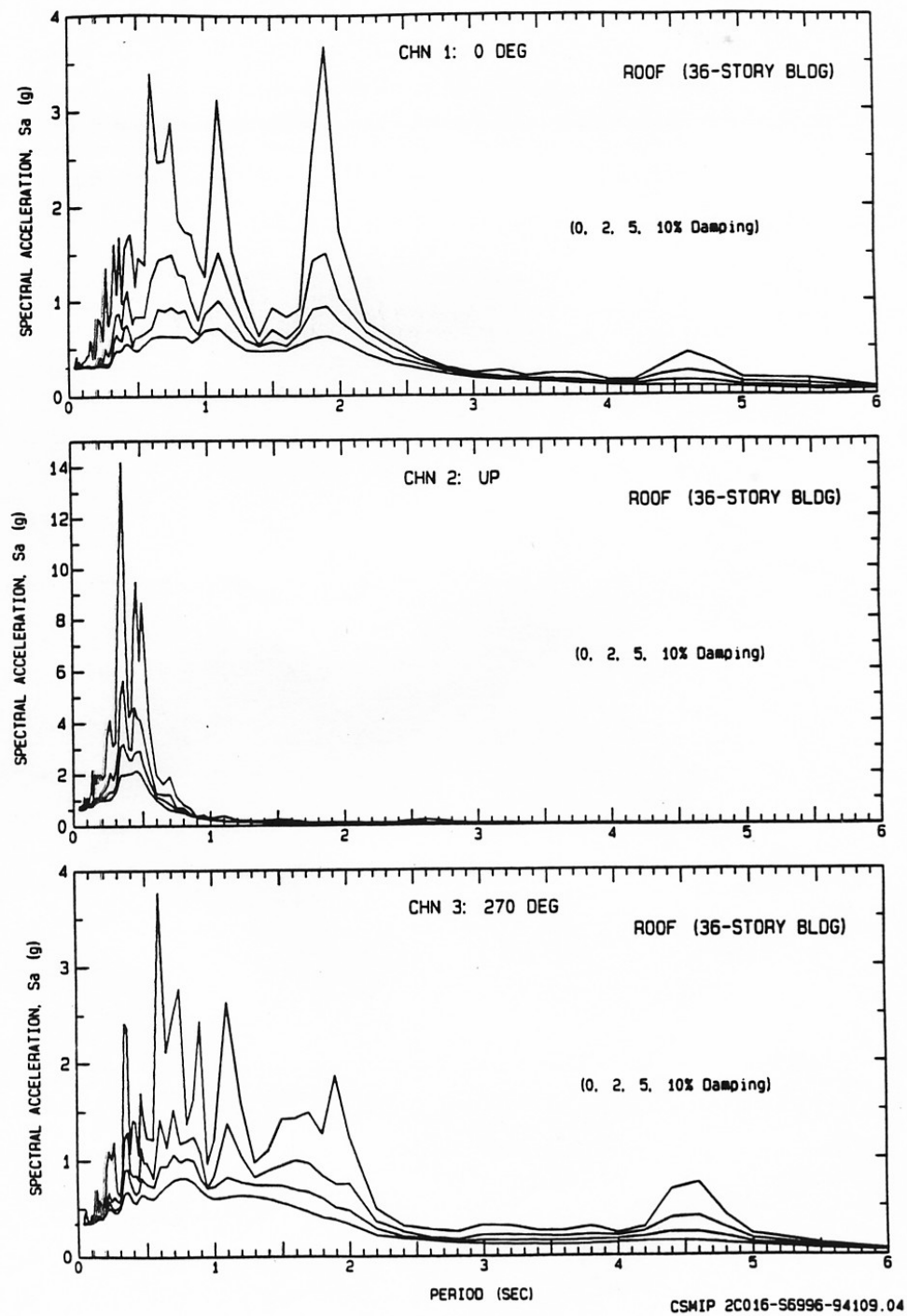
CSMIP 2C009-S5202-94116.03

NORTHRIDGE EARTHQUAKE OF JAN 17, 1994      CSMIP PRELIMINARY PROCESSING  
 LOS ANGELES - AVE OF THE STARS #2      CSMIP Sta Num 2C016  
 Usable Data Bandwidth: .17 to 23.6 Hz (.04 to 6.0 Sec)

15

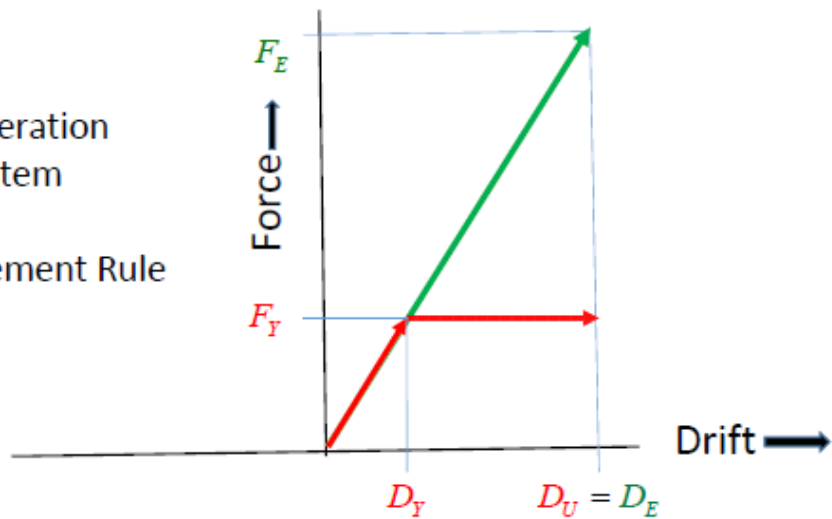


NORTHRIDGE EARTHQUAKE OF JAN 17, 1994 CSMIP PRELIMINARY PROCESSING  
LOS ANGELES - AVE OF THE STARS #2 Sta Num 2C016  
USABLE DATA BANDWIDTH: .17 TO 23.6 HZ (.04 TO 6.0 SEC)



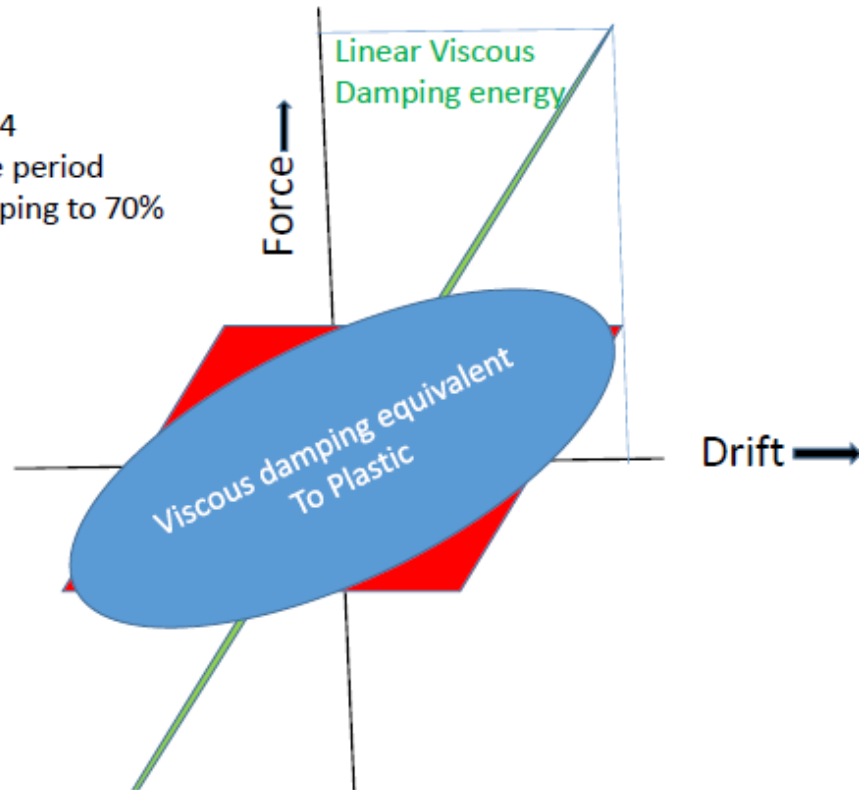
Spectral Acceleration  
For ductile system

Equal Displacement Rule



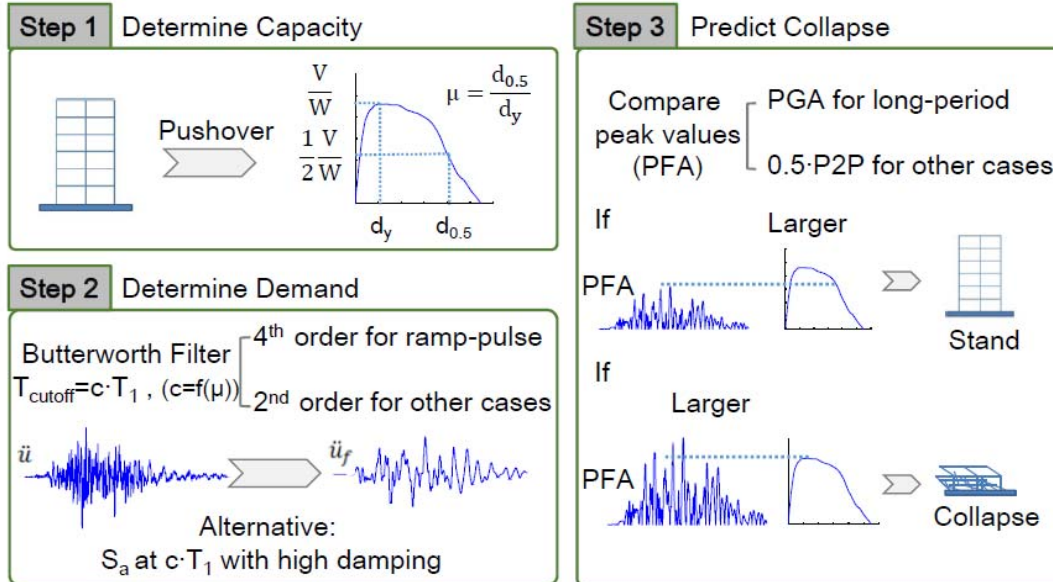
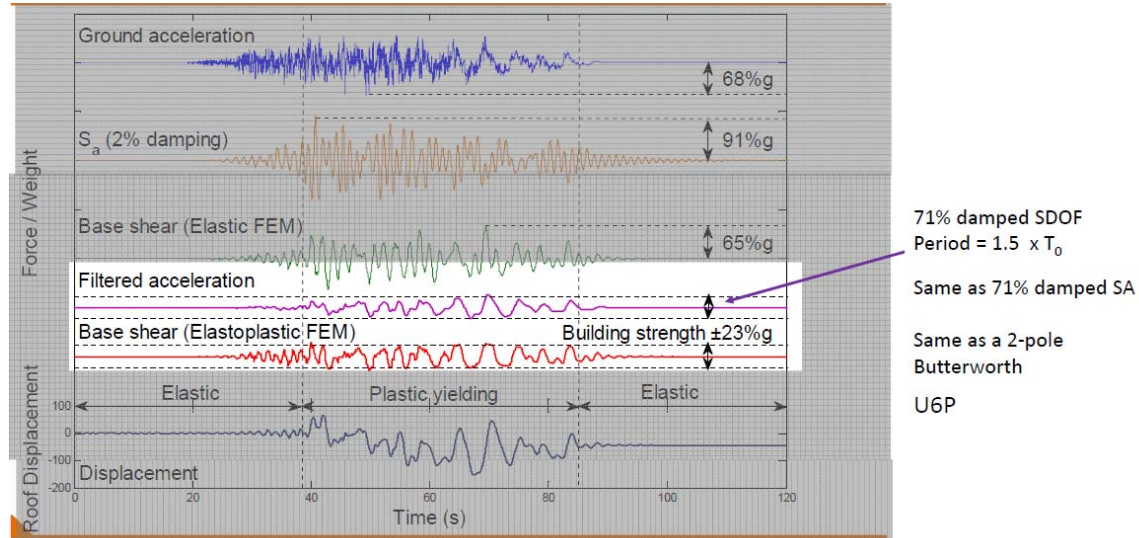
$$D_U = D_E \text{ when } R \text{ factor} \equiv \frac{F_E}{F_Y} = \frac{D_U}{D_Y} \equiv \text{ductility}$$

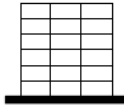
For an R-factor of 4  
Should double the period  
And increase damping to 70%



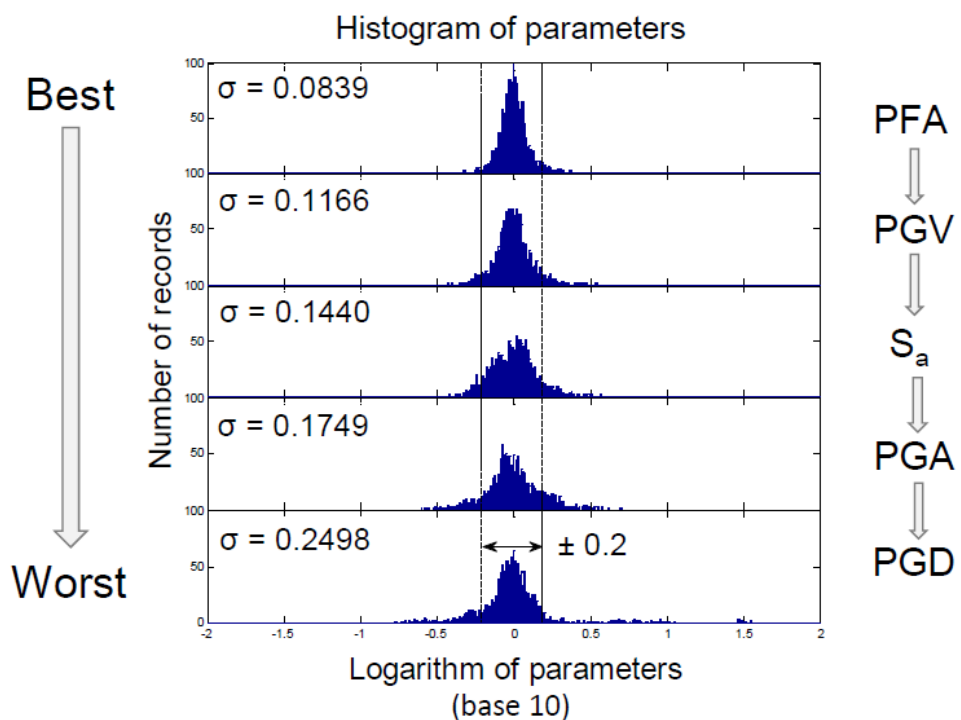
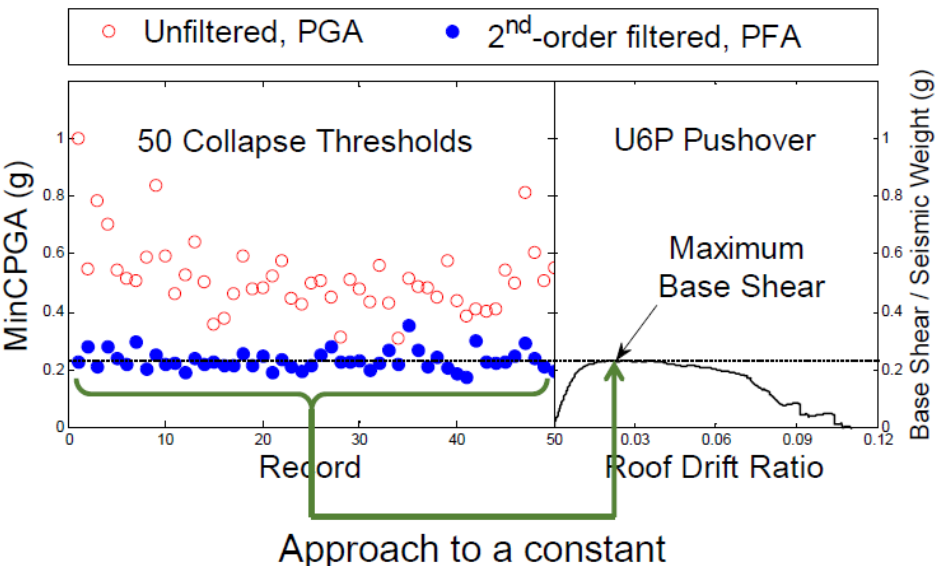
Building as single degree of freedom system. Traditionally buildings are approximated by a 5% damped oscillator at the linear frequency of the building (green). However, it is understood that they are more like an elasto-plastic sdof (red), where plastic yielding

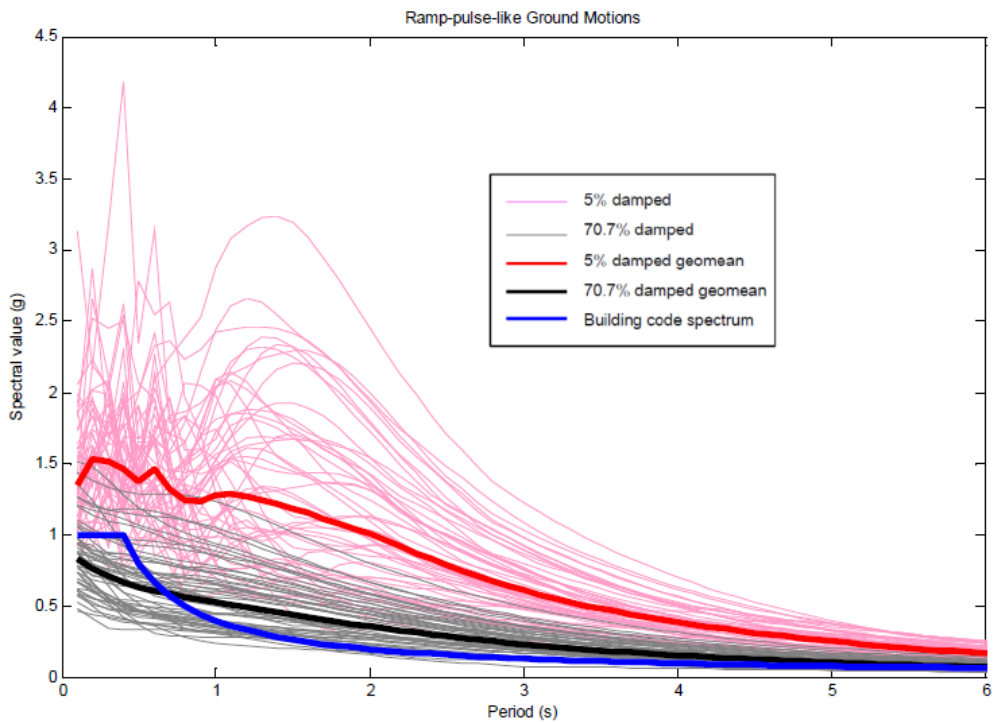
occurs at drift  $D_y$  and force  $D_y$ . The energy lost in a plastic cycle is the pink area in the parallelogram. If linear analysis is desired then it is more appropriate to simulate the plastic system with an equivalent linear system with longer period and much larger damping (the blue system).



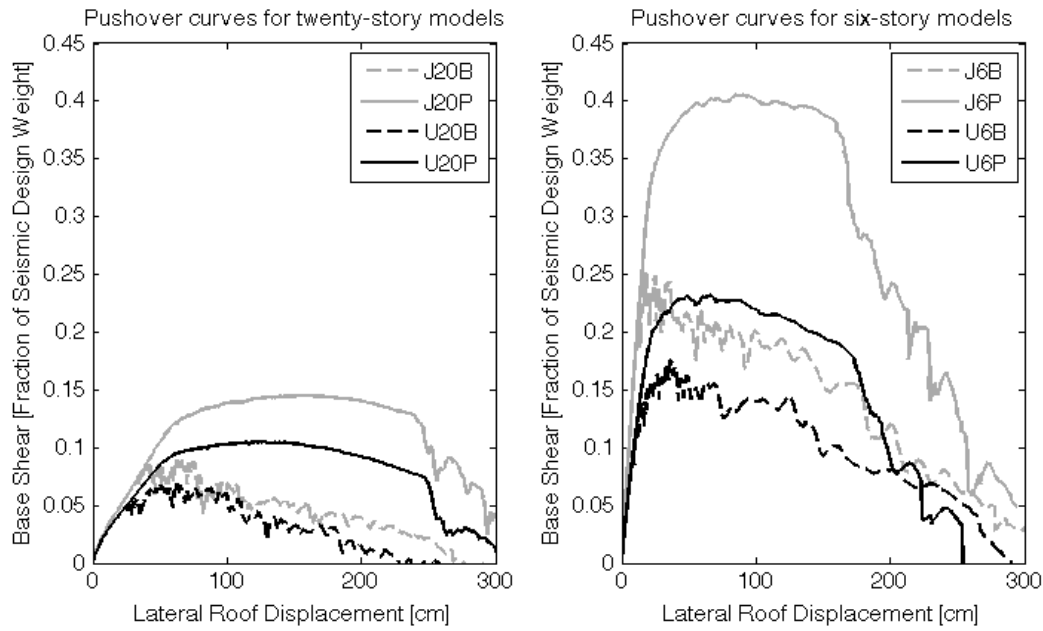


## U6P in Long-period Ground Motions





### Finite element analysis



Pushover curves for the twenty-story (left) and six-story (right) building models.

Pushover curves for the twenty-story (left) and six-story (right) building models.

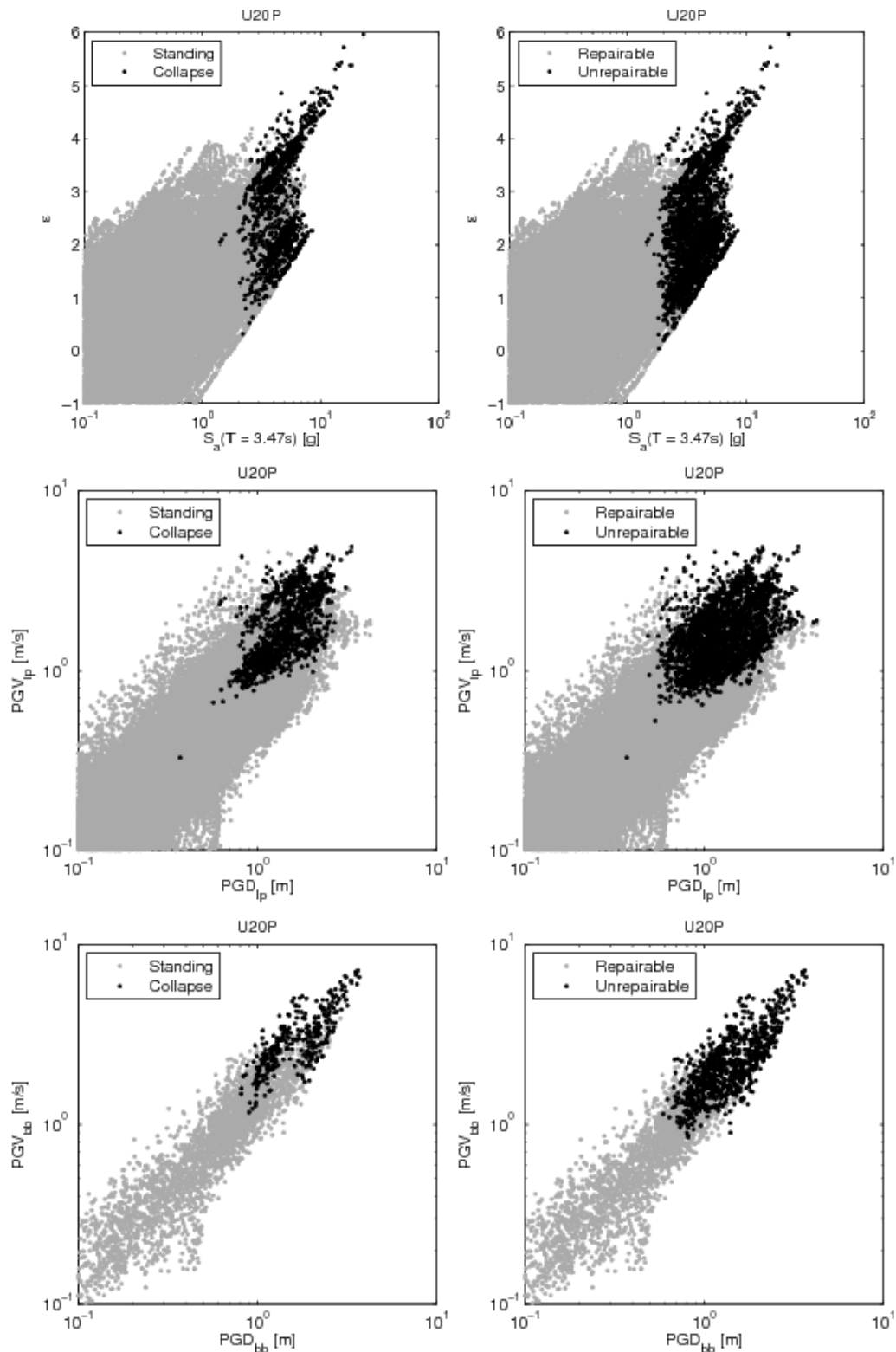


**Figure 2.** Data from simulations of the U20P building model response to long-period ground motions in the  $S_a$ - $\varepsilon$  (top row),  $\text{PGD}_{lp}$ - $\text{PGV}_{lp}$  (middle), and  $\text{PGD}_{bb}$ - $\text{PGV}_{bb}$  planes. The

building responses are: “standing” or “collapse” (left column) and “repairable” or “unrepairable” (right).

responses are: “standing” or “collapse” (left column) and “repairable” or “unrepairable” (right).

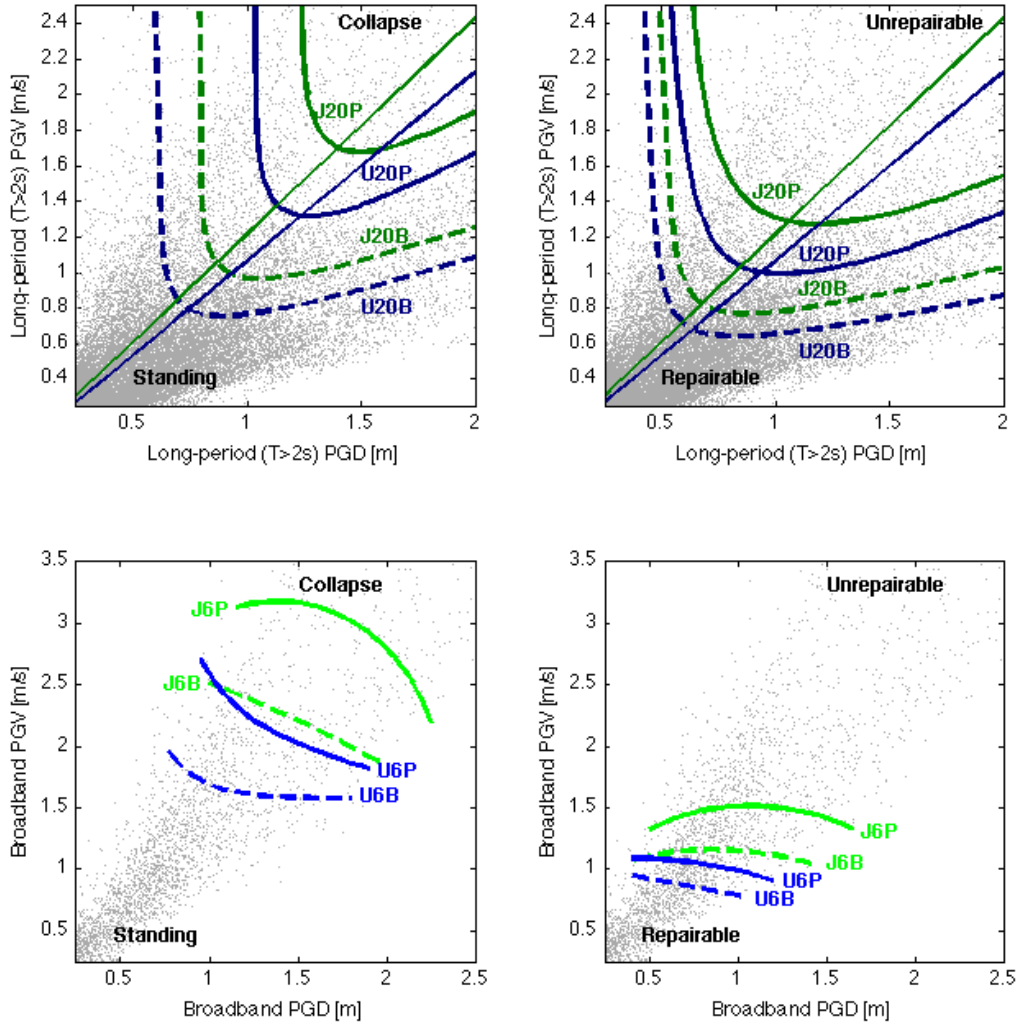
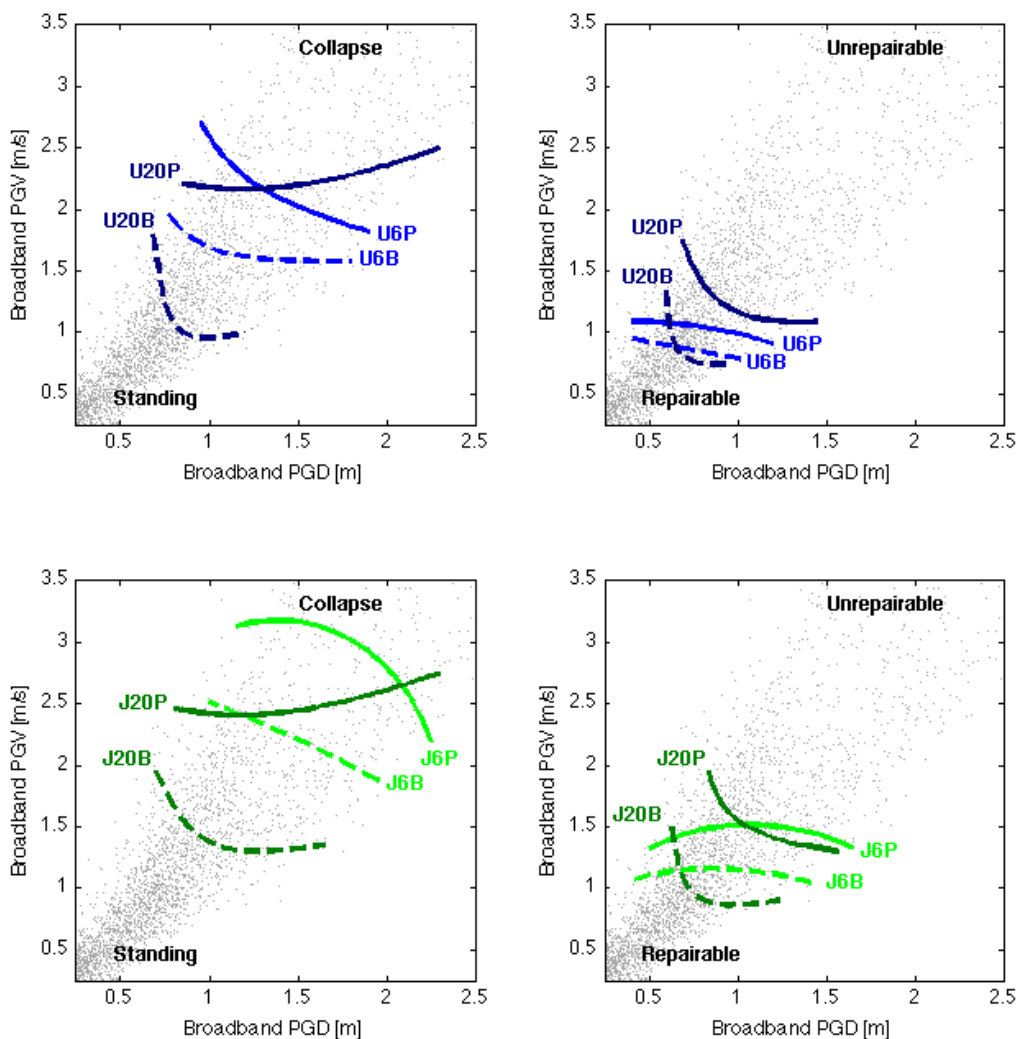
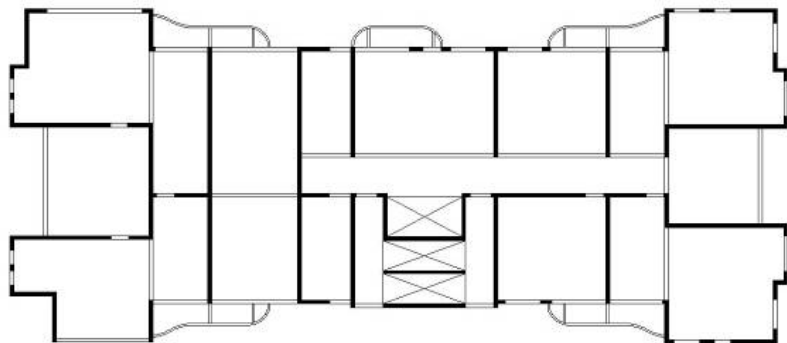


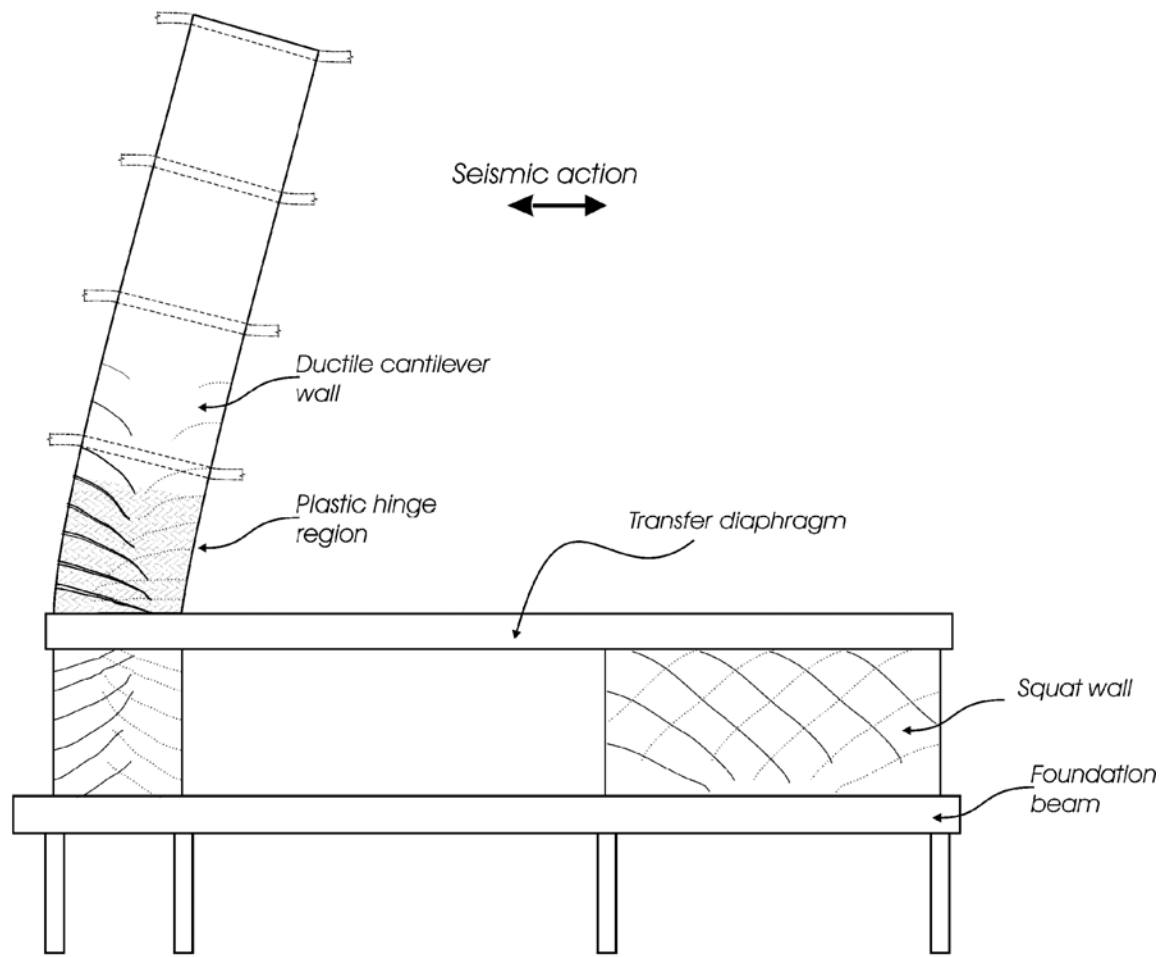
**Figure 3.** Contours where the probability of “collapse” (left) or “unrepairable” (right) is 30% for Model 22. The gray points are the PGD and PGV values of the long-period (top) and broadband (bottom) ground motions. The equivalent PGV<sub>bb</sub> is approximately  $1.5 \cdot \text{PGV}_{lp}$  with a standard deviation of 0.24 m/s. The diagonal lines in the top plots are  $\text{PGV}_{lp} = \frac{2\pi}{1.7T} \text{PGD}_{lp}$ , where  $T$  is the fundamental elastic period of the J20P or U20P building model.



Chile – a different approach





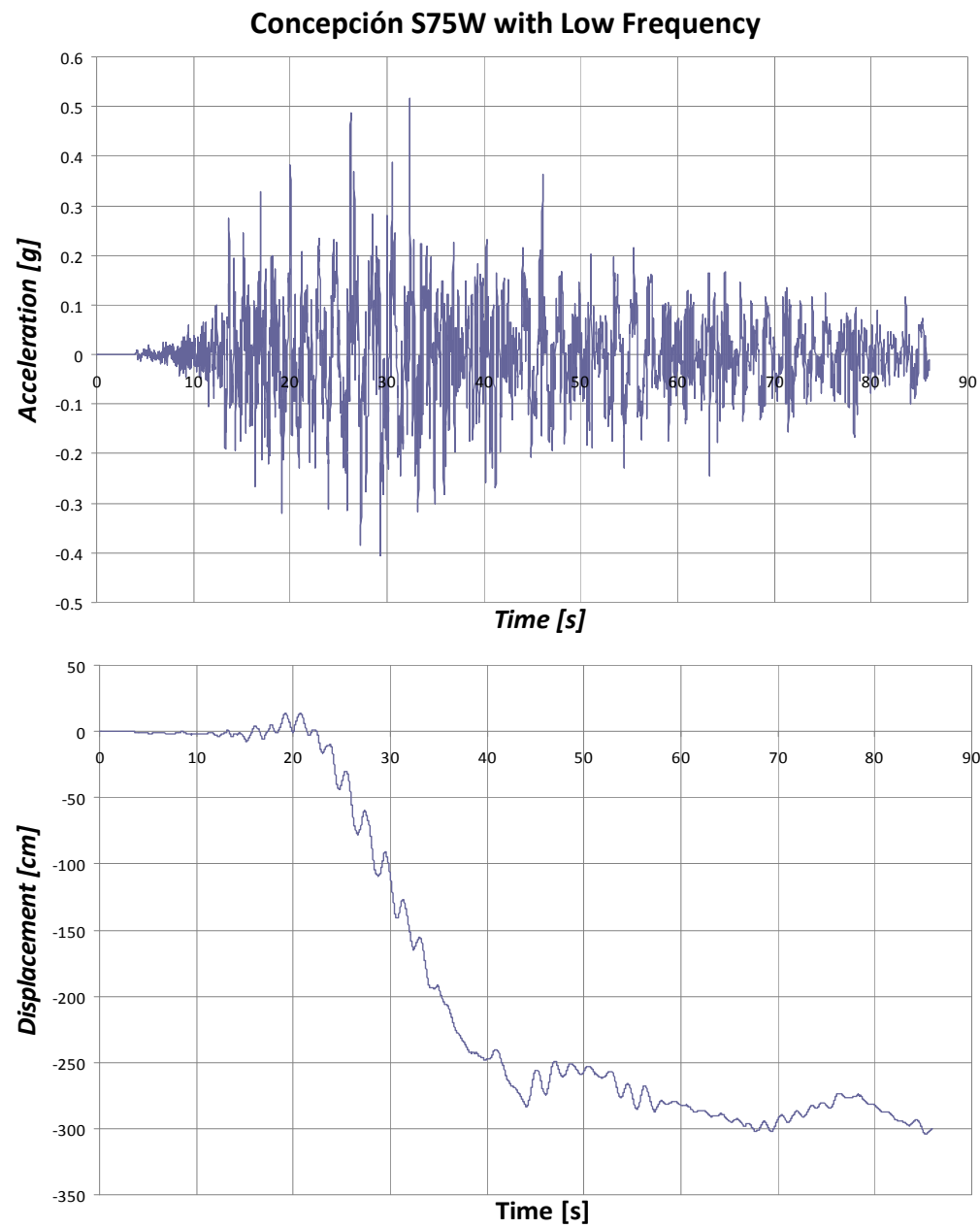




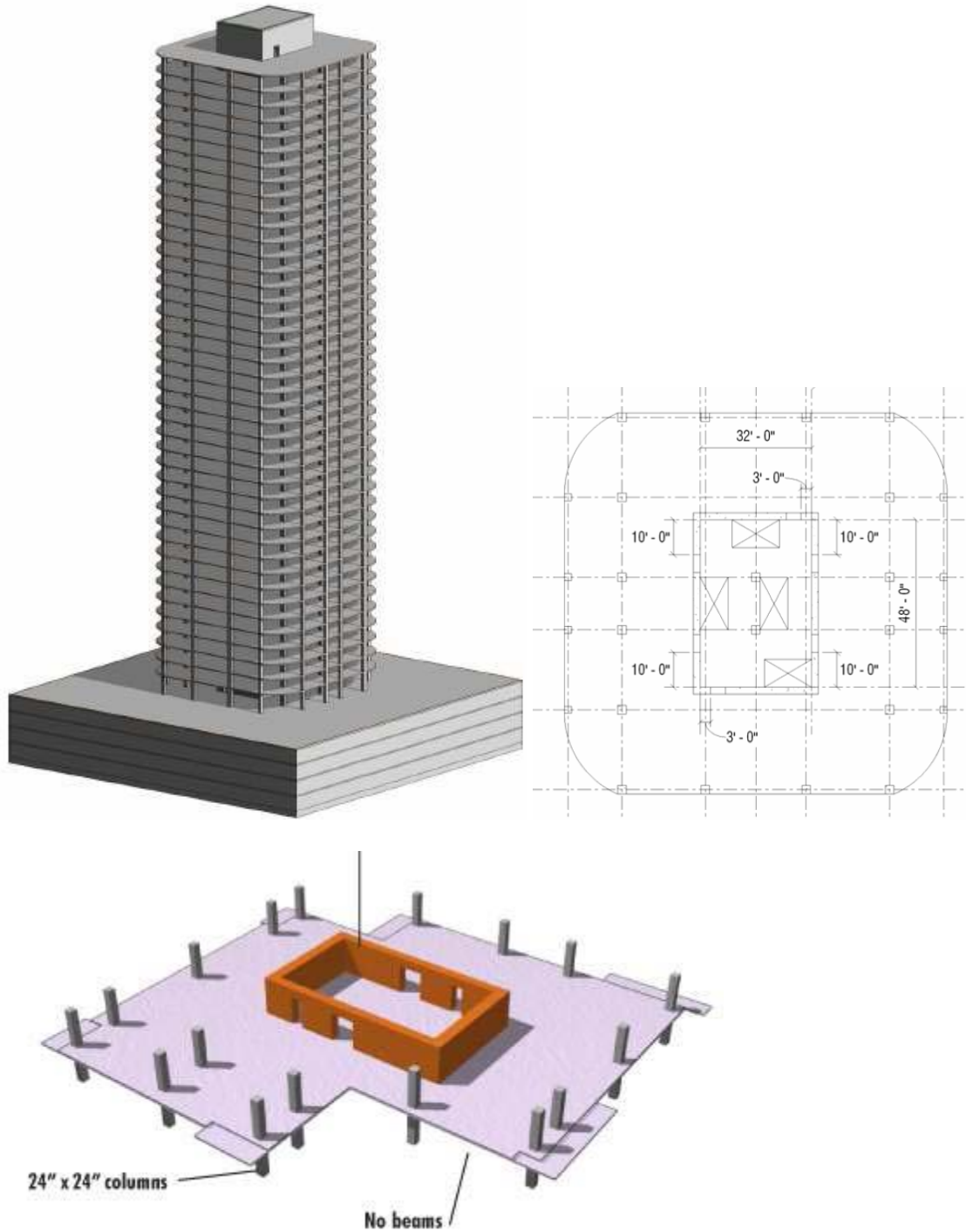
Shear failure in a new 25-story shear wall building in the 2010 Maule earthquake



Collapse of a shear wall building in the 2010 Maule earthquake



Core wall buildings



## Homework Chapter 6

1. Assume that the base of a shear-beam (neglect bending deformations) with rigidity  $\mu$  and density  $\rho$  is subject to tangential displacement that given by  $u_x(t)$ . Assume that the top of the shear beam is a free surface.

$$u_x(t) = \begin{cases} 0, & t < 0 \\ t, & t > 0 \end{cases}$$

- a) Write the motion of the free end of the beam as a function of time.
- b) Write the shear stress at the forced end of the beam as a function of time.
- c) How would this problem change if you were to allow bending deformations in the beam?